Surface Chemistry of Ketones and Diketones on Lewis Acidic γ-Al_2O_3 Probed by Infrared Spectroscopy

Bryan J. Hare[1], Ricardo A. Garcia Carcamo[2], Rachel B. Getman[2], and Carsten Sievers[1,*]

[1]School of Chemical and Biomolecular Engineering, Georgia Institute of Technology, Atlanta, GA 30332, United States

[2]Department of Chemical and Biomolecular Engineering, Clemson University, Clemson, SC 29634, United States

*Corresponding author: carsten.sievers@chbe.gatech.edu

Abstract

To advance the understanding of surface reactions of biomass-derived oxygenates, adsorption and conversion of ketones and diketones on Lewis acidic γ-Al_2O_3 is studied. The model compounds include ketones with hydroxyl groups (di/hydroxyacetone) as well as diketones with different distances between the two carbonyl groups (2,3 butanedione and 3,4 hexanedione, 2,4 pentanedione, and 2,5 hexanedione as α, β, γ diketones, respectively). In situ infrared (IR) spectroscopy is utilized to experimentally observe the surface species. The deconvoluted IR spectra acquired between 50 and 250 °C suggest that intermolecular aldol condensation is the most common reaction path for the studied di/ketone reagents. This reaction path consists of sequential enolization, dimerization, and dehydration to form conjugated products with lower ν(C=O) and ν(C=C) frequencies. Exceptions included intramolecular aldol condensation of 2,5 hexanedione and isomerization and dehydration of dihydroxyacetone. Density functional theory calculations suggest that diketones bind as monodentate surface species provided their stability on γ-Al_2O_3. This study provides insight on

di/ketone chemistry on Lewis acidic γ-Al_2O_3 that will be relevant for many fields including prebiotic and industrial chemistry.

Introduction

Ketones are an important class of organic reactants that are essential to the chemical industry. They serve as important precursors for the manufacturing of synthetic polymers,[1-2] enantiopure alcohols,[3] imines/amines,[4] and more. Diketones have also been utilized to synthesize specific compounds with high regio, diastereo, and enantioselectivity.[5-6] While ketones and diketones may be acquired through a variety of sources and synthesis processes, it is likely that heterogeneous acid-base catalysts, typically metal oxides, are involved in some stage of their production or conversion. Therefore, it is important to understand the surface reactions of di/ketones on metal oxides and how the exact structure of the reactant affects reactivity and the final products.

Many metal oxide catalysts exhibit Lewis acidity, which allows these materials to chemically adsorb both gas- and liquid-phase reactants. Lewis acidic γ-Al_2O_3 in particular has been extensively studied in regards to its microstructure, surface behavior, and role as a catalyst or support.[7-8] It is commonly utilized as a support for metal particles for a number of reactions in refineries and more sustainable chemical processes, including the Fischer-Tropsch process[9] and aqueous phase reforming.[10] γ-Al_2O_3 is also used as an acid catalyst for some processes including alcohol dehydration and the Claus process for desulfurization of natural gas.[11-12] Because these reactions are strongly tied to the petrochemical and biorefinery

industries, of which many di/ketones originate, better understanding the interactions between di/ketones and γ-Al_2O_3 is essential.

Acetone is the simplest of ketones and is historically the most commonly used ketone for deciphering how molecules with carbonyl groups bind and react on different surfaces including those of metallic single crystals and various metal oxide materials.[13-18] It is activated on Lewis acidic oxides, such as γ-Al_2O_3, to produce mesityl oxide through sequential enolization, aldol self-condensation and dehydration reactions.[19] However, the reactivity trends and surface phenomena of ketones, and certainly diketones, of varying characteristics (size, types of functional groups, distance between functional groups, etc.) have yet to be rationalized in a single study.

Several types of spectroscopy have been employed to probe the adsorption and surface chemistry of ketones, particularly acetone, on surfaces. For instance, infrared (IR) spectroscopy was used by Hanson et al. to observe the Lewis acid-catalyzed transformation of adsorbed acetone into its enol tautomer on γ-Al_2O_3.[20] It was also deduced in the same study that the enol species was responsible for initiating oligomerization with a nearby ketone species through a nucleophilic attack to form diacetone alcohol, an intermediate in mesityl oxide production. Qi et al. utilized nuclear magnetic resonance (NMR) spectroscopy to probe the activation of acetone on framework Sn-sites of Sn-β zeolites in the Meerwein-Ponndorf-Verley-Oppenauer reaction.[21] Furthermore, Senanayake et al. used both X-ray photoelectron spectroscopy (XPS) and near-edge X-ray adsorption fine structure spectroscopy (NEXAFS) to demonstrate the different binding orientations (η_1 or dioxypropylene) of acetone adsorbed on oxidized and reduced CeO_2 films.[22] Conner et al. used attenuation total reflection IR spectroscopy and a

direct comparison of vibrational frequencies to show that acetylacetone binds to a TiO_2 surface very similarly to that of an acetylacetone ligand in a Ti-based coordination complex.[23] These and many other studies have demonstrated the versatility and powerful nature of spectroscopy in revealing the surface chemistry of ketone functional groups on oxide surfaces. For theory-driven research, density functional theory has proven useful in calculating ketone adsorption parameters on metal oxide surfaces.[24] Some examples include adsorption energies and bond lengths of acetone on ZnO for sensing applications and activation energies for acetone and aldol condensation intermediates adsorbed to different sites on TiO_2 surfaces.[25-26] While some di/ketone chemistry on oxide surfaces has been studied with experiments or theory, studies including both approaches are much less common.

In this study, IR spectroscopy was used to observe surface reactions on γ-Al_2O_3. Adsorbed species included acetone and more complex di/ketone species that vary based on size, presence of alcohol groups, and distance between C=O groups. Temperature-programmed reaction/desorption experiments under high vacuum tracked the progression of Lewis acid site-catalyzed reactions on dry γ-Al_2O_3 as well as the general binding strength of surface species up to 250 °C. Deconvolution of the ν(C=O)/ν(C=C) region of the IR spectra (~1450 – 1800 cm^{-1}) revealed the vibrational modes of various intermediates and products formed from surface reactions. Configurations and relative binding energies for adsorbed diketones were acquired via density functional theory.

Methods

Experimental

Powdered γ-Al_2O_3 (Alfa Aesar 99.97%) was used as the adsorbent material. All the di/ketone reagents used in this study are listed in **Table 1** with Lewis structures and vendor information.

Table 1. Ketone and diketone reagents used to observe Pt deactivation

Reagent name	Lewis structure	Notes	Vendor information
Acetone	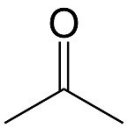	Simplest ketone	Alfa-Aesar, HPLC Grade 99.5+%
Hydroxyacetone	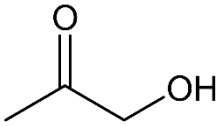	Ketone with 1 neighboring OH group	Alfa Aesar, 95%
Dihydroxyacetone	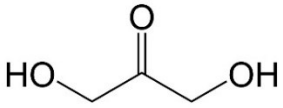	Ketone with 2 neighboring OH groups	Sigma-Aldrich (for synthesis)
Mesityl Oxide	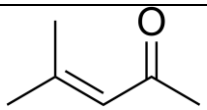	Forms from acetone self condensation	Sigma-Aldrich, ≥97.0% (for synthesis)
2,4-pentanedione	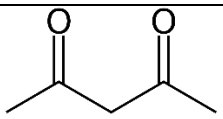	β-diketone	Sigma-Aldrich, ReagentPlus® ≥99%
2,5-hexanedione	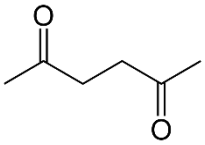	γ-diketone	Sigma-Aldrich, ≥98%
2,3-butanedione	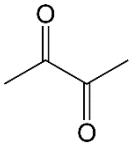	Small α-diketone	Sigma-Aldrich, 97%
3,4-hexanedione	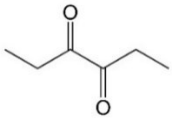	Large α-diketone	Sigma-Aldrich, ≥95%

Adsorption of volatile di/ketones (every reagent listed in **Table 1** except DHA and 25HD) was performed under high vacuum (HV) with hydraulically pressed self-supporting wafers comprised of ~10 – 20 mg of γ-Al_2O_3 powder. The wafers were first activated under HV at 450 °C (10 °C/min) for 1 h to desorb residual water and other contaminants. IR spectra were acquired using a Thermo Scientific Nicolet 8700 FT-IR spectrometer that contained an MCT-A detector. Each spectrum collected was an average of 64 scans, each taken with an optical velocity of 1.8988 and a resolution of 1.928 cm^{-1}. After obtaining a spectrum for activated γ-Al_2O_3, the wafer was exposed to ~0.5 mbar of the di/ketone vapor at 50 °C for ~15 min. This would result in the formation of various IR bands attributed to both strongly chemisorbed surface species as well as weakly physisorbed species with liquid-like characteristics that make up multilayers. The chamber was then evacuated to achieve HV conditions prior to beginning the temperature-programmed desorption (TPD). This would cause a notable decrease in the intensity of bands associated with physisorbed species., suggesting that some desorption took place and that chemisorbed species dominated the surface. Herein, the wafer temperature was ramped (10 °C/min) to 100, 150, 200, and 250 °C. After each temperature was maintained for ~15 min, the wafer was allowed to cool naturally to 50 °C, so that all spectra in the TPD experiments were obtained at the same temperature. The spectrum of activated γ-Al_2O_3 was subtracted from other spectra obtained throughout the TPD experiments to isolate absorbance bands that corresponded to surface species derived from di/ketone adsorption and reactions. All IR spectroscopy data was processed with Thermo Scientific Omnic software.

The adsorption of non-volatile di/ketones (DHA and 25HD) was also probed under HV. However, a different approach for adsorption was necessary given the insufficient vapor

pressures. About 50 mg of γ-Al_2O_3 was impregnated with 2,5 hexanedione or a 1% (w/w) aqueous solution of dihydroxyacetone until the sample appeared saturated. The sample was then maintained under vacuum over night. The sample was ground into a powder that was pressed into a self-supporting wafer and positioned within the same HV IR cell. The wafer was allowed to sit in HV at ambient temperature for 2 h to remove physisorbed species prior to the aforementioned TPD experiment procedures, excluding the initial activation at 450 °C.

Features in the acquired IR spectra were deconvoluted using a custom Python code.[27] An exponential baseline was calculated while the band shape was assumed to exhibit a PseudoVoigt profile (i.e. a combination of 50 % Gaussian and 50 % Lorentzian characteristics).

Computational

The γ-Al_2O_3 surface was built by cleaving a (100) surface facet from the bulk structure of a γ-Al_2O_3 obtained from Digne,[28] which has a space group of P21/m and calculated lattice parameters of a = 5.6 Å, b = 8.4 Å and c = 8.1 Å and angles of α = β = γ =90°. The simulation supercell (**Figure S1**) is a 2 × 2 × 2 expansion of the unit cell with the surface in the c direction and is periodic with dimensions of a = 16.2 Å, b = 16.8 Å and c = 35.5 Å and α = β = γ =90°. 25 Å of vacuum space are included between vertical images. Gas phase molecules were simulated in a box with dimensions 20 × 20.1 × 20.2 Å.

DFT calculations were performed using the Vienna Ab initio Simulation Package (VASP)[29-33] using PAW pseudopotentials[34-35] to an energy cutoff of 400 eV and the PBE exchange correlation functional.[36] D3 dispersion with Becke-Jonson damping[37-38] was included, spin

polarization was turned on, and dipole corrections were applied in the direction normal to the surface. The first Brillouin zones were sampled using 3 × 3 × 1 Monkhorst–Pack Gamma-centered k-point meshes[39] in the case of alumina slab structures and 1 × 1 × 1 k-point meshes in the case of gas molecules. Electronic structures were calculated self-consistently until the difference in energy between subsequent iterations was no larger than 10^{-6} eV. Geometries were considered converged when the magnitudes of the forces on all atoms fell below 0.03 eV/Å in geometry optimizations. Acetone was used as a common energy reference which also provided insight to the influence of sterics for diketone binding energies. The binding energies were calculated and referenced to adsorbed acetone according to **Equation 1**

$$\mathbf{E_{Relative\ Binding}} = \mathbf{E_{Adsorbed\ molecule*}} - \mathbf{E_{Gas\ phase\ molecule}} - \mathbf{E_{Adsorbed\ acetone}} - \mathbf{E_{Gas\ phase\ acetone}} \quad \mathbf{(1)}$$

Where $\mathrm{E_{Adsorbed\ molecule*}}$ is the DFT-calculated energy of the adsorbed species, $\mathrm{E_{Adsorbed\ acetone}}$ is the energy of adsorbed acetone, $\mathrm{E_{Gas\ phase\ molecule}}$ is the energy of the gas phase molecule, and $\mathrm{E_{Gas\ phase\ acetone}}$ is the energy of gas phase acetone. The different adsorbed molecule structures were generated from an initial configuration based on the gas phase molecule geometry. Adsorption into both tetrahedral and octahedral sites was tested. Different orientations of the adsorbate with respect to the surfaces were tested; specifically, horizontal, tilted, and vertical molecule orientations were tested (see Supporting Information **Figure S2**). The structures reported herein are those that give the lowest energies.

Results

The same batch of γ-Al_2O_3 used herein was characterized in a previous study, exhibiting a BET surface area of 63 m^2/g and a Lewis acid site concentration of 72 μmol/g that could retain adsorbed pyridine at 250 °C.[40] IR spectra were first acquired for low pressures of vapor phase di/ketones that exhibited sufficient volatility for a strong signal **(Figure S3)** and general vibrational mode assignments for distinct IR bands below 1800 cm^{-1} in the IR spectra of the free molecules are listed in **Table S1**. This excludes dihydroxyacetone and 2,5 hexanedione. The full IR spectra of γ-Al_2O_3-adsorbed di/ketones are presented in **Figure S4.** Features representing various molecular vibrational modes were observed in the 1000 – 4000 cm^{-1} range. This includes aliphatic C-H stretching, C=O stretching, CH_x deformation, and C-O stretching modes typically found within 2700 – 3000, 1550 – 1900, 1150 – 1500, and 1000 – 1300 cm^{-1}, respectively.[41]

Bands attributed to γ-Al_2O_3-adsorbed species generally exhibit increased broadness due to adsorption to Al^{3+} sites with a wide variety of coordination and acidity. Theoretically, overtone bands for ν(C=O) and ν(C=C) vibrational modes could be observed in the 3200 – 3500 cm^{-1} region, exhibiting around twice the frequency of their respective fundamental bands. However, given the presence of a large, broad feature in the region attributed to hydrogen bonding and the significant diversity of surface species in most experiments, no apparent overtone bands attributed to particular surface species were observed. Therefore, spectral deconvolution was conducted only for the ~1500 – 1800 cm^{-1} region. The IR spectrum of activated γ-Al_2O_3 contained small bands at 3765 and 3727 cm^{-1} associated with surface hydroxyl groups on tetrahedrally and octahedrally coordinated Al^{3+} sites, respectively.[42] These bands

diminished rapidly during the adsorption of di/ketones. This suggested that di/ketones either displaced or perturbed (via hydrogen bonding) surface hydroxyls, the latter resulting in broadening and a shift to lower frequencies. However, this distinction could not be made based on the experimental evidence. The large, broad feature (2750 – 3750 cm^{-1}) attributed to hydrogen bonding hydroxyl species was observed during the adsorption of each di/ketone, suggesting a notable extent of hydrogen bonding in each experiment due to surface and interadsorbate interactions between a wide variety of species. Thus, this region was not deconvoluted.

Mesityl Oxide and Acetone

Mesityl oxide adsorption on γ-Al_2O_3 **(Figure 1a)** gave rise to a strong feature within the 1500 – 1750 cm^{-1} region. While the IR spectrum of the free vapor phase molecule **(Figure S3a)** contained two strong, distinct features centered at about 1704 and 1634 cm^{-1} for the ν(C=O) and ν(C=C) modes, respectively, the broadness in this region exhibited during adsorption suggests that there may be distinct surface species or perhaps the same species adsorbed to different sites. It was previously shown that ν(C=O) and ν(C=C) frequencies of mesityl oxide on zeolites are generally higher when adsorbed to Lewis acid sites as opposed to surface hydroxyl groups.[43] As sites become decreasingly Lewis acidic, the shifts of both IR bands are expected to be nearly equivalent given the conjugation within the C=C-C=O system.[44] These conclusions also imply that the conjugated isomer is dominant on the γ-Al_2O_3 surface with little, if any, contributions from the non-conjugated isomesityl isomer that ordinarily makes up about 10%

of a solution.[45] Thus, the 1500 – 1750 cm^{-1} feature was deconvoluted into 4 main bands at 1670, 1625, 1599, 1570 representing ν(C=O) on Lewis sites, ν(C=O) on hydroxyl groups, ν(C=C) on Lewis sites, and ν(C=C) on hydroxyl groups (**Figure 1a)**, respectively. The weaker high frequency contribution centered at 1700 cm^{-1} is likely due to a weakly physisorbed species.[43] These, and all other assignments **(Table 2)**, were made under the assumption that all adsorbed species retained the conjugated isomeric structure.

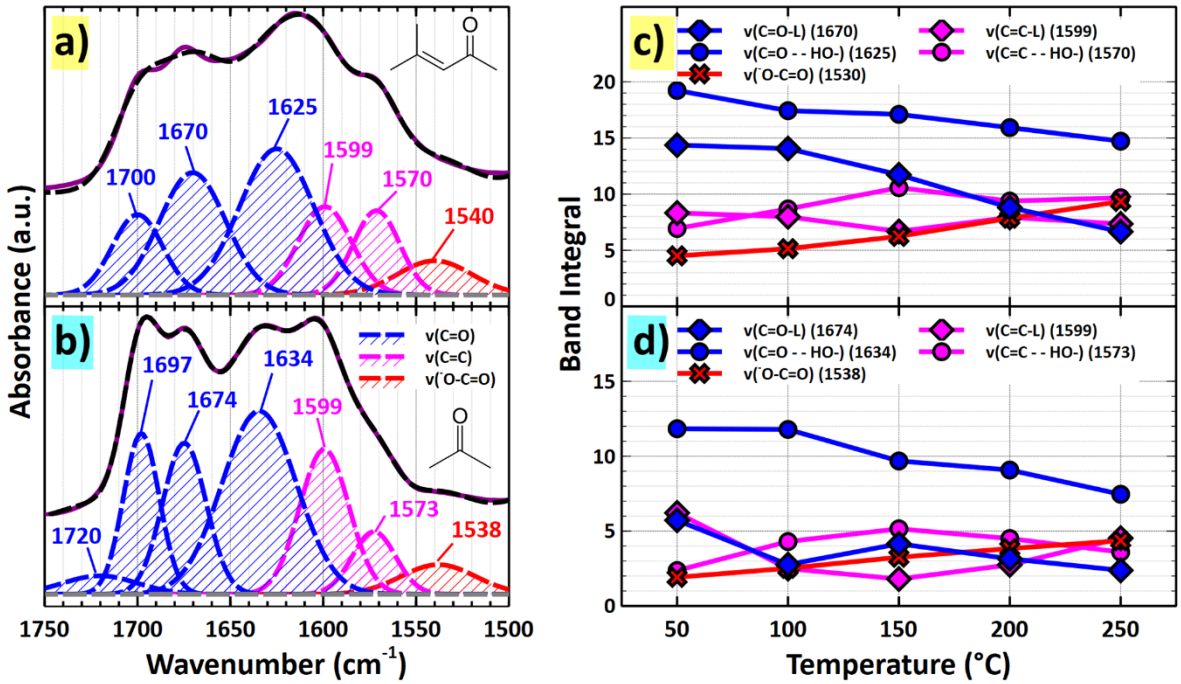

Figure 1. Deconvolution of the 1500 – 1750 cm^{-1} region of IR spectra for adsorbed **a)** mesityl oxide and **b)** acetone at 50 °C and **c,d)** corresponding temperature-dependent band integrals up to 250 °C. Mesityl oxide and acetone-related data is highlighted in yellow and light blue, respectively.

The adsorption of acetone **(Figure 1b)** presents a very similar set of spectra as that of mesityl oxide. It is well known that strong Lewis acid sites, such as those on γ-Al_2O_3, facilitate the aldol condensation of acetone into diacetone alcohol.[46] This intermediate then undergoes dehydration to form mesityl oxide **(Scheme 1)**. While a further extent of aldol condensation to

form phorone, isophorone, and mesitylene products is possible,[47] no IR bands affiliated with these species were observed. All general assignments for IR bands observed below 1800 cm^{-1} during mesityl oxide and acetone adsorption are listed in **Table 2**.

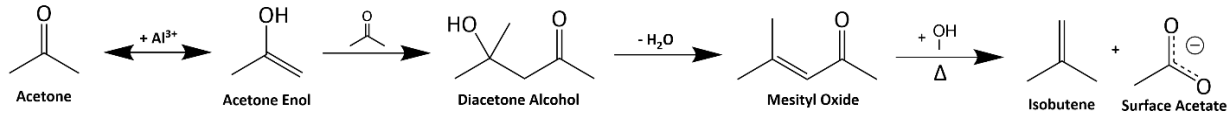

Scheme 1. Acetone and mesityl oxide reactions on γ-Al_2O_3 up to 250 °C under HV

The region of 1500 – 1750 cm^{-1} was deconvoluted to acquire individual IR bands for ν(C=O) and ν(c=C) modes **(Figure 1a,b)**. Bands associated with physisorbed mesityl oxide (1700 cm^{-1}) and acetone (1720 and 1697 cm^{-1}) were present at 50 °C but decreased in intensity with increasing temperature. When comparing the remainder of the deconvoluted region, individual bands associated with adsorbed mesityl oxide share similar frequencies to those observed during acetone adsorption. This may suggest that γ-Al_2O_3 converts a significant fraction of adsorbed acetone into mesityl oxide even at a temperature as low as 50 °C. Because no IR bands associated with the acetone enol tautomer nor the diacetone alcohol intermediate were detected, it also implies that the reaction occurs faster than the accumulation of the IR spectra. Results from an additional 10 min kinetics experiment corroborated this theory **(Figure S5)**. The exposure of γ-Al_2O_3 to acetone vapor instantaneously resulted in a large band at 1700 cm^{-1} which grew for 30 s. At this point, the band began displaying a severe decrease in intensity up to 10 min at which the system was evacuated. Bands associated with adsorbed mesityl oxide concomitantly grew and became dominant. It is therefore suggested that the surface coverage on γ-Al_2O_3 is dominated by mesityl oxide even during acetone adsorption.

Changes in band integrals within the 1500 – 1750 cm^{-1} region after heating to different temperatures reflect the conversion of surface species **(Figure 1c,d)**. For instance, as the temperature increased, the band integrals for ν(C=O) modes appeared to decrease, while those of ν(C=C) modes remained relatively constant. This could be associated with the growth of the small band at 1538 – 1540 cm^{-1} during both mesityl oxide and acetone adsorption. We attribute this band to the ν($^{-}$O-C=O) mode of a surface acetate formed along with isobutene during the fragmentation of mesityl oxide **(Scheme 1)**, typically initiated via a nucleophilic attack of the carbonyl carbon by the hydroxyl group of an adjacent enol.[43] We would expect any isobutene produced to desorb from the surface given low temperatures previously reported to be required to observe any notable adsorption in the IR spectrum.[48] Although small, the band grew somewhat in size as the temperature increased, signifying a higher extent of conversion.

Table 2. IR band assignments for acetone and mesityl oxide adsorption on γ-Al_2O_3 under HV at 50 – 250 °C. Arrows depict frequency shifts at higher temperatures.

General vibrational mode	Acetone Adsorption				Mesityl Oxide Adsorption		
	Acetone	Mesityl Oxide	Acetate	Notes	Mesityl Oxide	Acetate	Notes
ν(C=O)	1720			Physisorbed acetone			
	1697 → 1692			Physisorbed acetone	1700		Physisorbed MSO
		1675 → 1670		MSO on Lewis acid site	1670		MSO on Lewis acid site
		1634 → 1625		H-bonded MSO	1625		H-bonded MSO
ν(C=C)		1599 → 1595		MSO on Lewis acid site	1599 → 1596		MSO on Lewis acid site
		1573		H-bonded MSO	1570		H-bonded MSO
ν($^-$O-C=O)		1538	1538	MSO-derived acetate		1540	MSO-derived acetate
δ(CH)		1477	1477			1475	
		1453 → 1457			1452 → 1455		
		1427 → 1424			1421		
	1378 → 1387				1385 → 1388		
	1363 → 1365				1364 → 1366		
		1332 → 1335			1323 → 1331		
		1320 → 1310			1311		
π(CH)		1287			1284 → 1281		
		1264			1258		
	1234 → 1229				1230 → 1238		
		1200			1208 → 1214		
		1193			1191		
	1171						
		1151			1147		

Hydroxyacetone

Upon hydroxyacetone adsorption to γ-Al_2O_3, a dominant band emerged at 1718 cm^{-1} and was assigned to the ν(C=O) mode of the adsorbed species. This band was

accompanied by a low frequency shoulder and a tailing feature that extended as low as 1500 cm^{-1}, which required deconvolution **(Figure 2a)** and integration of the bands **(Figure 2b)**. The 1718 cm^{-1} band remained dominant but steadily decreased with increasing temperature up to 250 °C, suggesting there may be desorption or a possible a surface reaction. The slight countering growth of bands at 1675, 1645, 1588, and 1531 cm^{-1} **(Table 3)** implied that not only did a reaction occur, but there were multiple distinct products that likely exhibited alkene characteristics.

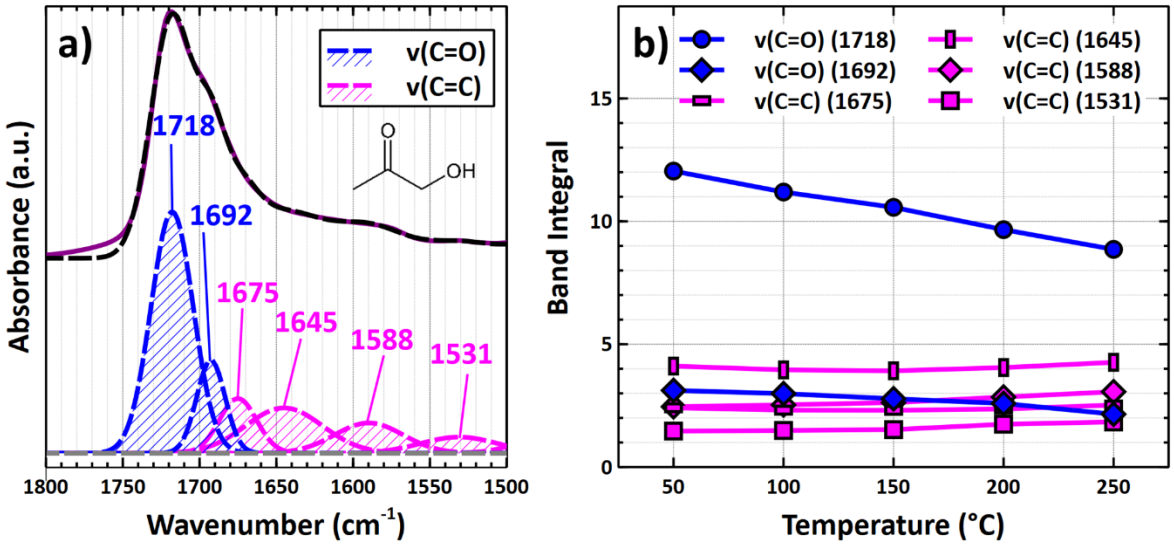

Figure 2. a) Deconvolution of the 1500 – 1800 cm^{-1} region of the IR spectrum of adsorbed hydroxyacetone on γ-Al_2O_3 at 50 °C. **b)** Corresponding temperature-dependent band integrals up to 250 °C.

Hydroxyacetone tautomerization could in principle result in a combination of two different enol products.[49] The cleavage of a C-H bond on the hydroxyl or methyl carbons initializes formation of prop-1-ene-1,2 diol and prop-2-ene-1,2 diol, respectively.[50] These surface species will simply be referred to as enediols. The ν(C=C) modes of the enediols were assigned to the 1675 and 1645 cm^{-1} bands. Given their lack of intramolecular conjugation, they

should accommodate the higher frequency ν(C=C) bands. In addition, the 1,2 enediol should exhibit a higher ν(C=C) frequency because it possesses two hydroxyl groups directly attached to the alkene group as opposed to only one on the 2,3 enediol.[41] Therefore, the 1675 and 1645 cm^{-1} bands were assigned to the 1,2 and 2,3 enediols, respectively.

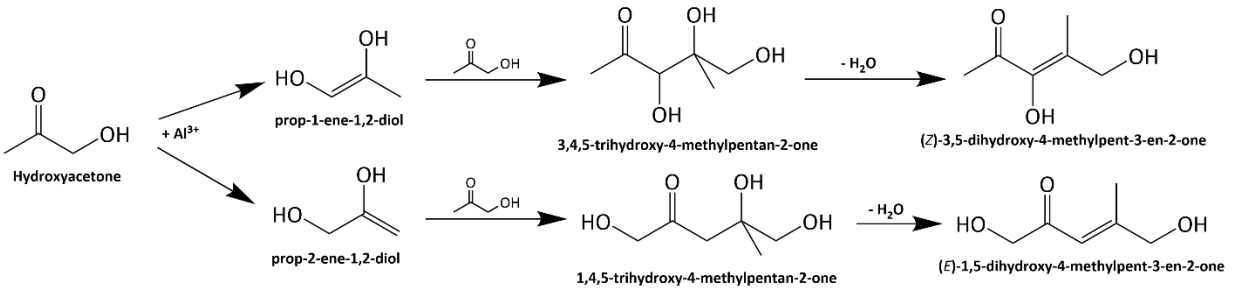

Scheme 2. Hydroxyacetone reactions on γ-Al_2O_3 up to 250 °C under HV

The remaining bands at 1692, 1588, and 1531 cm^{-1} were assigned to species formed from aldol condensation of adsorbed hydroxyacetone. We attributed the 1692 cm^{-1} band to a ν(C=O) mode and because of its lower frequency (in comparison to 1718 cm^{-1}), it was likely associated with a conjugated surface species. The bands at 1588 and 1531 cm^{-1} were thus assigned to two different ν(C=C) modes. With two different enediols on the γ-Al_2O_3, there should be two different aldol condensation products formed upon reaction with molecular hydroxyacetone. The nucleophilic attack of the carbonyl should produce a dimeric intermediate that is dehydrated to form the final conjugated product **(Scheme 2)**. Therefore, conversion of the 1,2 and 2,3 enediols should produce 3,5 dihydroxy-4-methylpent-3-en-2-one (35DH) and 1,5 dihydroxy-4-methylpent-3-en-2-one (15DH), respectively. There were likely two ν(C=C) bands given that the hydroxyl groups are located on different carbon atoms. Similar to the enediols, we suspect the 35DH product will exhibit a higher ν(C=C) frequency since both

hydroxyl groups are directly bonded to the alkene group. As a result, we assigned the 1588 and 1531 cm^{-1} bands to the 35DH and 15DH condensation products, respectively.

Table 3. IR band assignments for hydroxyacetone adsorption on γ-Al_2O_3 under HV at 50 – 250 °C. Arrows depict frequency shifts at higher temperatures.

General vibrational mode	Hydroxyacetone	1,2 enediol	2,3 enediol	3,5 dihydroxy condensation product	1,5 dihydroxy condensation product	Notes
ν(C=O)	1718					
				1692		May also include 1,5 dihydroxy condensation product
ν(C=C)		1675				
			1645			
				1588		
					1531	
δ(CH)				1456		
	1425					
				1375		
	1357					
				1333		
π(CH)	1270 → 1265					
				1232		
	1219					
	1194					
	1172					
	1155					

Dihydroxyacetone

Because the adsorption of dihydroxyacetone was performed ex-situ in the aqueous phase, contributions from γ-Al_2O_3 were not subtracted from the IR spectra **(Figure 3)**. Although this made deconvolution of the mid IR region more difficult, notable features in the ν(C=O) region were still identified. In addition, a separate TPD experiment with H_2O adsorbed to γ-Al_2O_3 was performed **(Figure S6)** to isolate the spectral contributions from small amounts of co-

adsorbed H_2O. The main band of interest located within the 1630 – 1650 cm^{-1} region was attributed the δ(HOH) mode of molecular H_2O.

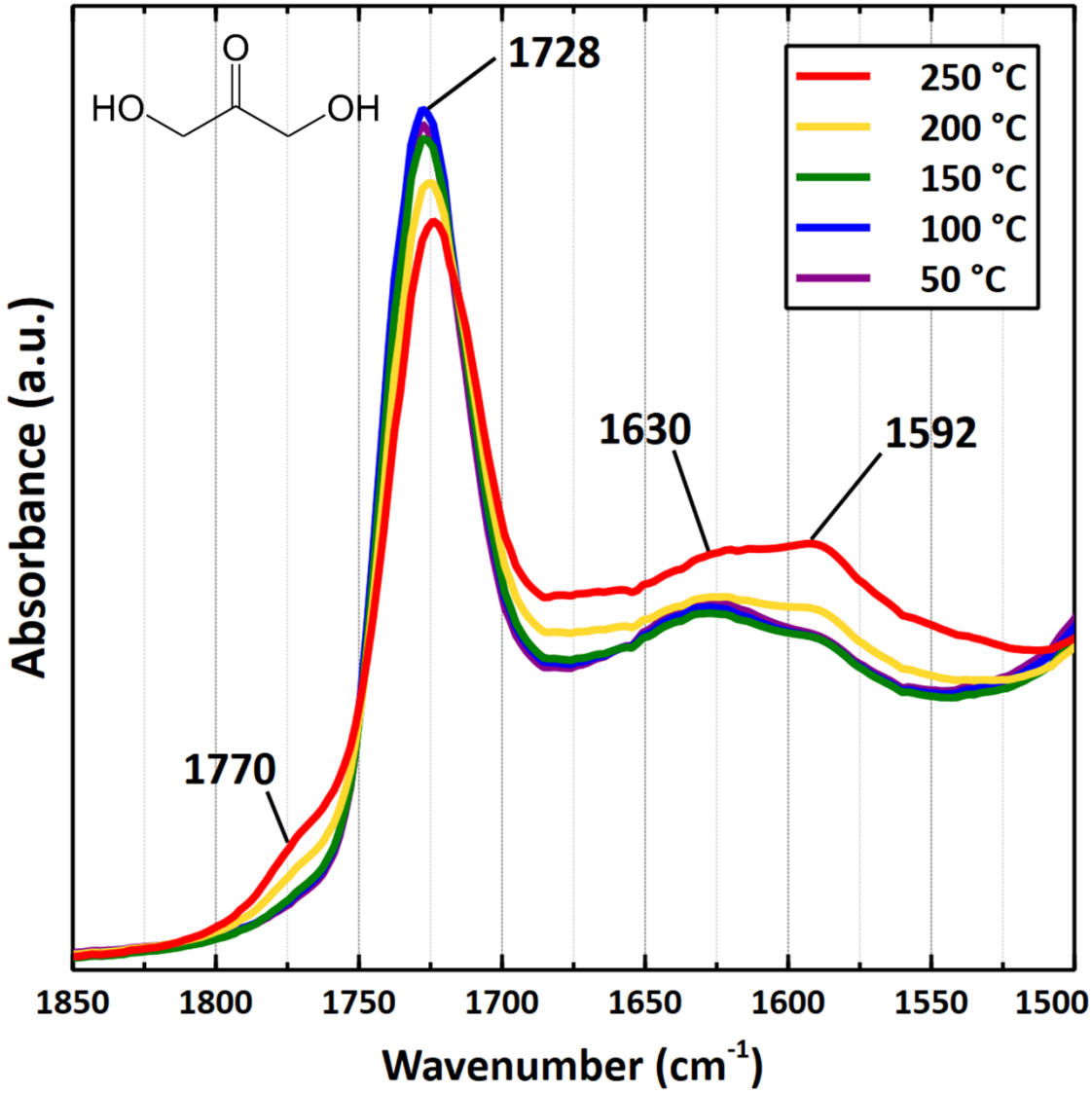

Figure 3. Infrared spectra (ν(C=O) region) of surface species formed from dihydroxyacetone on γ-Al_2O_3 (prepared in the aqueous phase) during TPD experiments from 50 to 250 °C.

The large feature at 1728 cm^{-1} was associated with the ν(C=O) mode of adsorbed dihydroxyacetone. While this band remained dominant, it did exhibit a slight decrease in intensity up to 250 °C. This development was perhaps related to an equal enlargement of low

frequency bands at 1630 and 1592 cm^{-1} and the appearance of a new high-frequency shoulder at 1770 cm^{-1}, each of which suggest a surface reaction occurred. The bands at 1630 and 1592 cm^{-1} were assigned to the v(C=O) modes of the aldehyde and ketone group, respectively, of adsorbed pyruvaldehyde. Dihydroxyacetone conversion into pyruvaldehyde has been previously demonstrated on Lewis acidic materials.[51-52] This was confirmed by a separate TPD experiment in which pyruvaldehyde was adsorbed on γ-Al_2O_3 **(Figure S7)**. Herein, the same bands at 1630 and 1592 cm^{-1} were present and remained stable up to 250 °C. The high frequency shoulder that extended as high as ~1775 cm^{-1} that accompanied these bands may explain the development of the small feature identified herein at 1770 cm^{-1}. This tail is believed to represent the partial strengthening of (C=O) bonds of adsorbed pyruvaldehyde species that are more distant from surface hydroxyls and adsorbed H_2O. On γ-Al_2O_3, dehydration of dihydroxyacetone into pyruvaldehyde appears to be the dominant reaction **(Scheme 3)** with no observable evidence of enolization and condensation.

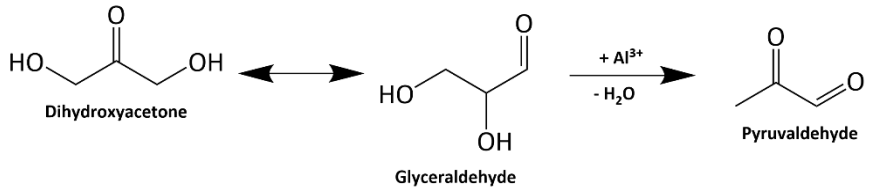

Scheme 3. Suggested reactions of dihydroxyacetone on γ-Al_2O_3.

2,4 Pentanedione

2,4 pentanedione, the enol tautomer, and the chelating ligand are illustrated in **Scheme 4** and are herein referred to as 24PD, Hacac, and acac, respectively, throughout interpretation of IR spectra during adsorption. Temprado et al. reported that the enol tautomer accounts for

81 mol% in a pure liquid phase at ambient temperature and contemplated a higher fraction in the pure vapor phase due to its greater volatility than that of the keto tautomer.[53] This was reflected by the dominating ν(C=O) band at 1637 cm^{-1} in the vapor phase spectrum **(Figure S3d)** and must be strongly considered during the interpretation of the IR spectra of the adsorbed species.

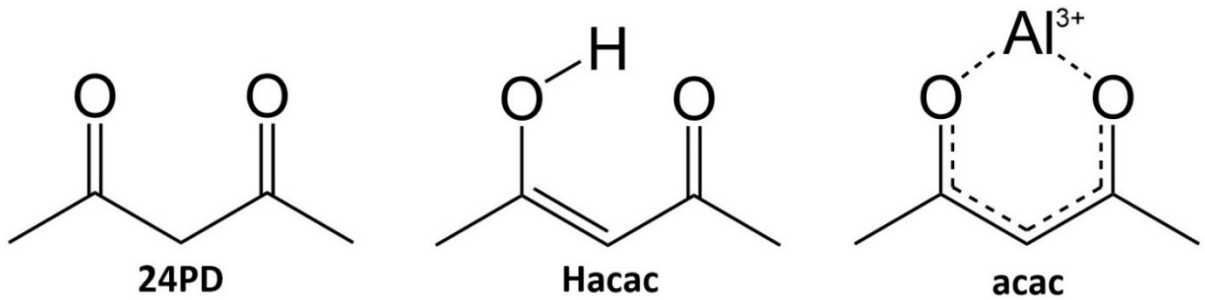

Scheme 4. Nomenclature for species derived from 2,4 pentanedione.

The deconvoluted IR spectra of 24PD/Hacac **(Figure 4a)** showed various individual features within the region of 1500 – 1750 cm^{-1}, including dominant bands centered at 1597 and 1533 cm^{-1}. ν(C=O) bands with lower frequencies within the 1500 – 1600 cm^{-1} are typically characteristic of carbonyl groups with bond orders of ~1.5 due to mesomerism and strong binding.[41] In addition, the 1300 – 1750 cm^{-1} region remained largely unchanged up to 250 °C, suggesting the surface species were extremely stable. Therefore, we assigned the 1597, 1533, and several other bands below 1750 cm^{-1} **(Table 4)** to an $Al(acac)_x$ surface species that dominated coverage on γ-Al_2O_3.[54-56]

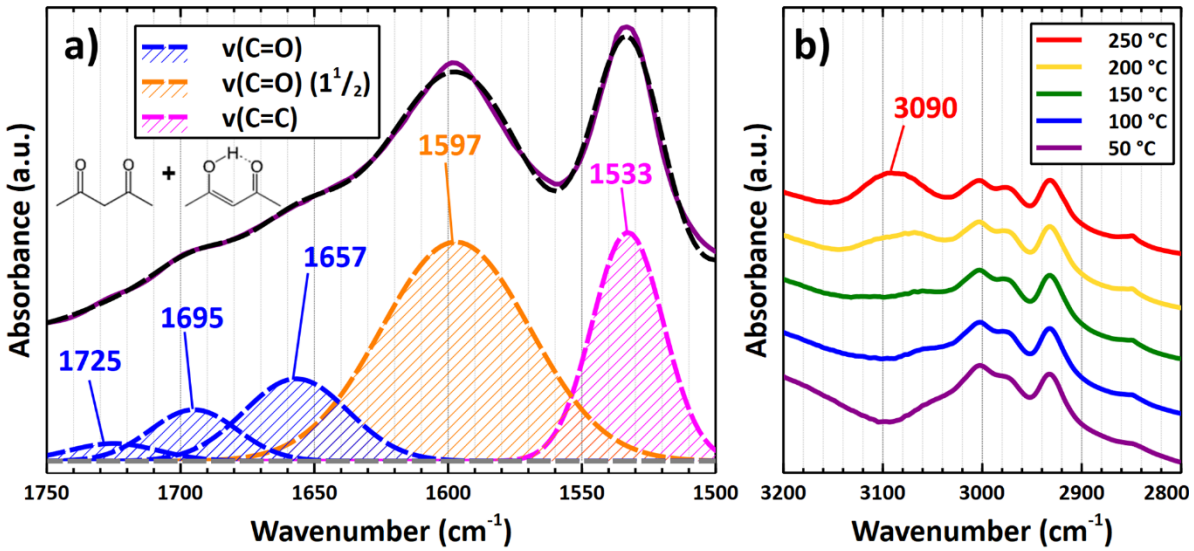

Figure 4. a) Deconvolution of the 1500 – 1750 cm^{-1} region of the IR spectrum of adsorbed 24PD/Hacac on γ-Al_2O_3 at 50 °C. **b)** Development of the ν(CH) stretching region during the TPD experiment.

While they exhibited notable thermal stability, adsorbed Hacac/acac species were not entirely resistant to surface-catalyzed reactions. For instance, Kytökivi et al. noticed the emergence of small IR bands at 1330 and 1055 cm^{-1} during the adsorption of 24PD/Hacac on γ-Al_2O_3 at 200 °C and claimed that these are affiliated with an acetate species resulting from molecular fragmentation, perhaps due interactions with surface hydroxyls or co-adsorbed H_2O.[54] These same bands, although small, were observed herein (1329 and 1055 cm^{-1}) at temperatures as low as 50 °C with slight growth up to 250 °C. The frequency of 1329 cm^{-1} is consistent with the ν(O=C-O) mode of acetic acid.[41] In this case, the formation of a surface acetate on γ-Al_2O_3 via Hacac/acac fragmentation should be concomitant with acetone production **(Scheme 5)**.

Table 4. IR band assignments for 2,4 pentanedione adsorption on γ-Al_2O_3 under HV at 50 – 250 °C. Arrows depict frequency shifts at higher temperatures.

General vibrational mode	2,4 pentanedione or Hacac	Acac (as $Al(acac)_x$)	Acetic acid	Notes
ν(C=O)	1725			Could also be physisorbed acetone
	1695			Could also be physisorbed acetone
	1657			
ν(C=O)		1597		Bond order of ~1.5
ν(C=C)		1533		
δ(CH_x)		1455		
		1396		
		1362 → 1360		
ν(O=C-O)			1329	
ν(C-CH_3)		1293 → 1296		
	1250			
π(CH3)		1192		
ν(C-O)			1055	
ρ(CH_3)		1025		

While little temperature-dependency was seen in the low frequency region, a notable observation was made in the ν(CH) region between 2800 and 3200 cm^{-1} **(Figure 4b)**. From 50 to 150 °C, there were multiple bands within 2900 – 3050 cm^{-1} that remained constant. A band at 3090 cm^{-1} emerged at 200 °C and grew further at 250 °C. This band is assigned to the ν(CH) mode of an olefinic surface species.[41] While the free Hacac molecule is olefinic, the bidentate acac ligand of $Al(acac)_x$ is mesomeric and therefore demonstrates less of this characteristic due to electron delocalization. Given the unchanged low frequency absorbance, we believe the emergence of this band at 3090 cm^{-1} is due to the transition of a bidentate acac surface species to a monodentate Hacac species in which the C=C-H bonds are much more stable **(Scheme 4)**. This may be the first step in the thermal decomposition mechanism of $Al(acac)_3$ and the creation of a surface species that perhaps may subsequently react with surface hydroxyl groups

or another monodentate Hacac species to form acetates and 3,5-dimethylphenol, respectively; the latter product requiring higher temperatures (> 300 °C) than those used in this study.[57-58]

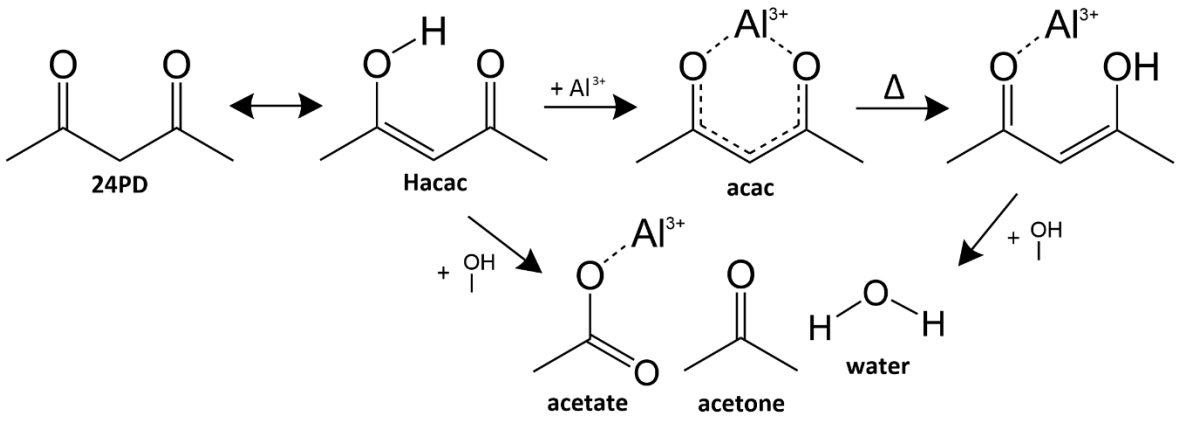

Scheme 5. 24PD/Hacac reactions on γ-Al_2O_3 up to 250 °C under HV.

2,3 Butanedione and 3,4 Hexanedione

α-Diketones such as 2,3 butanedione and 3,4 hexanedione contain two adjacent carbonyl groups. Up to 250 °C, the IR spectra of surface species from these molecules **(Figures S4f and S4g, respectively)** shared similar features in the 1600 – 1800 cm^{-1} region representing both ν(C=O) and ν(C=C) modes. However, major changes in band integrals were seen for those within the IR spectra of adsorbed 2,3 butanedione, while those of adsorbed 3,4 hexanedione demonstrated remained almost unchanged in the 50 – 250 °C temperature range. Band deconvolution was therefore necessary to isolate different species and rationalize the surface chemistry. Band frequencies for adsorbed α-diketones are listed in **Table 5**.

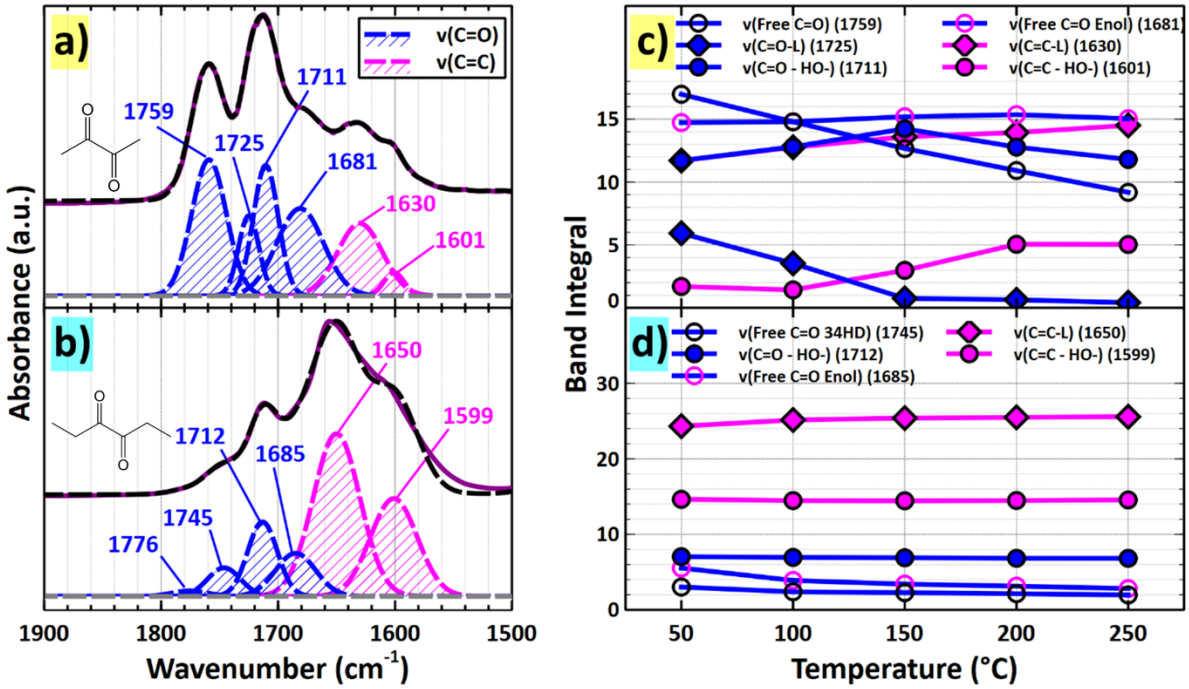

Figure 5. Deconvolution of the 1500 – 1800 cm^{-1} region of the IR spectrum of adsorbed **a)** 2,3 butanedione and **b)** 3,4 hexanedione on γ-Al_2O_3 at 50 °C and **c,d)** corresponding temperature-dependent band integrals up to 250 °C. 2,3 Butanedione and 3,4 hexanedione-related data is highlighted in yellow and light blue, respectively.

For vapor-phase 2,3 butanedione, one band at 1729 cm^{-1} represented the asymmetric ν(C=O) mode of the free molecule **(Figure S3e)**.[59] While adsorbed on γ-Al_2O_3, there was a large, dominating band at ~1712 cm^{-1} with shoulders, while a slightly smaller higher frequency band was observed at 1759 cm^{-1}. When comparing these frequencies with those of the vapor-phase spectrum, the bands of the adsorbed species suggest that one carbonyl group was elongated and weakened, while the other was contracted and strengthened, respectively. This suggests that the band at 1759 cm^{-1} represents the ν(C=O) mode of the free carbonyl group of 2,3 butanedione adsorbed in a monodentate orientation. The sharpness of this band, at least at lower temperatures, could corroborate this assignment, especially when compared directly to broader bands assigned to vibrational modes that more strongly interact with the γ-Al_2O_3

surface. A similar conclusion was made in a study regarding diketone adsorption on SiO_2 submerged in a CCl_4 solution.[60] In addition, multiple individual bands appeared to contribute to the band at 1712 cm^{-1}, which suggests that the carbonyl was bound to various distinct surface sites. The deconvoluted bands at 1725 and 1711 cm^{-1} **(Figure 5a)** are assigned to the ν(C=O) modes of 2,3 butanedione bound to Lewis acid sites and surface hydroxyl groups, respectively. Similar conclusions were made with mesityl oxide, another stable ketone species, as shown above and in another study.[44]

Individual bands were also observed within the 1600 – 1700 cm^{-1} region, suggesting that a species with a C=C bond had formed. These individual features are assigned to an enol surface species derived from 2,3 butanedione on Lewis acid sites. Herein, a distinct band for the free carbonyl group was identified at 1681 cm^{-1}, a much lower frequency perhaps due to a conjugated interaction with the vinyl C=C bond. Unlike acetone, 2,3 butanedione did not immediately undergo enolization during adsorption at 50 °C, but rather the decrease in band integrals associated with the diketone species **(Figure 5c)** may suggest that the acid-catalyzed tautomerization reaction occurred more readily at higher temperatures. However, the band integrals of enol bands remained relatively constant during the TPD.

Similar deconvolution results and conclusions were made for 3,4 hexanedione, the larger α-diketone. The ν(C=O) modes for the free carbonyl and the carbonyl bound to surface hydroxyls were centered at 1745 and 1712 cm^{-1}, respectively. The most noticeable differences between the spectra of adsorbed 3,4 hexanedione and those of 2,3 butanedione were the dominating band at 1650 cm^{-1} **(Figure 5b)**, the lack of temperature-dependency for the band integrals **(Figure 5d)**, and the lack of changes in the 1480 – 1580 cm^{-1} region at higher

temperatures. The dominating band at 1650 cm^{-1} was attributed to the ν(C=C) mode of the enol species adsorbed to Lewis acid sites while the smaller band at 1685 cm^{-1} was associated with the free conjugated carbonyl of this species. This suggested that 3,4 hexanedione enolized much more readily compared to 2,3 butanedione.

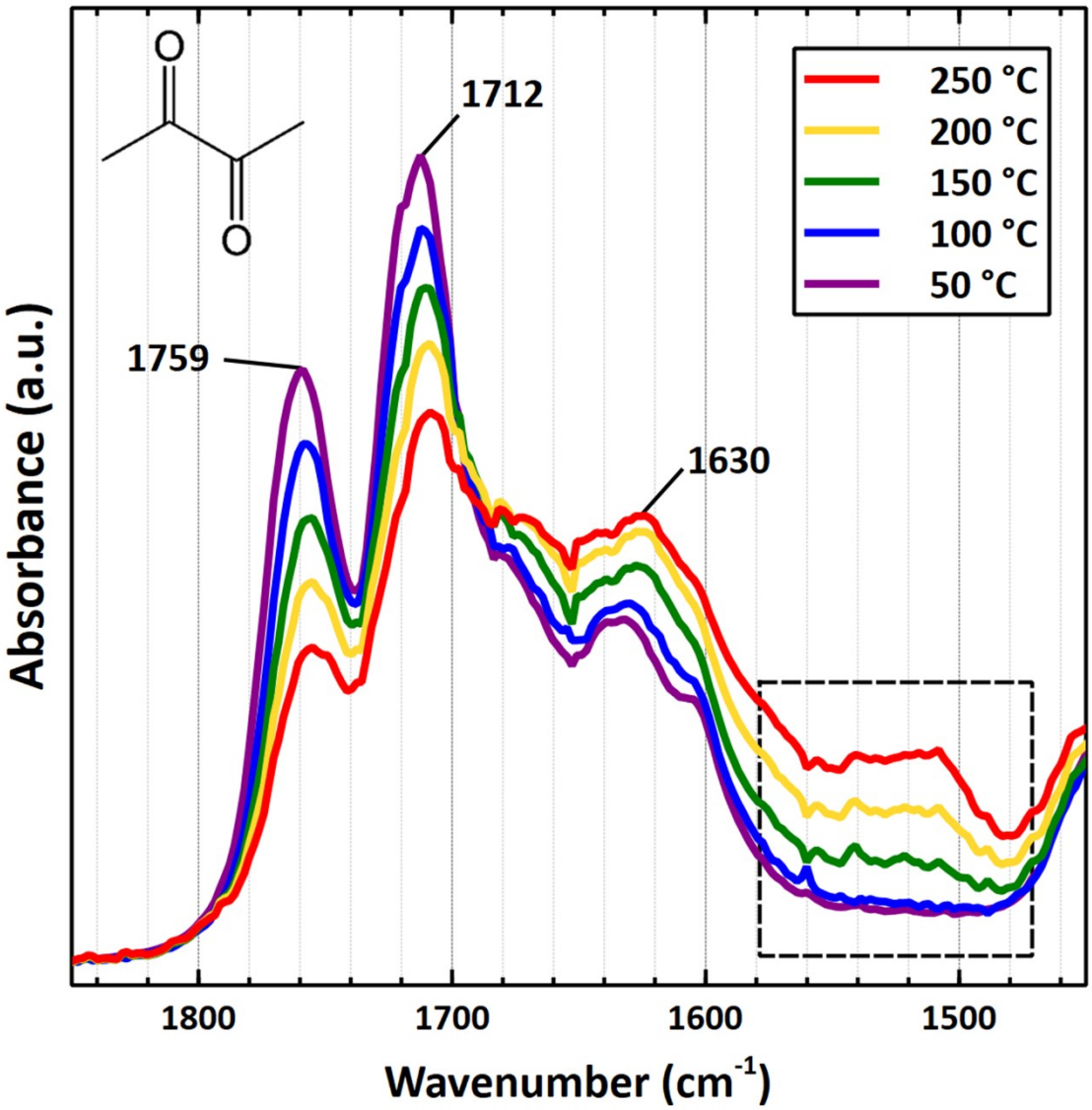

Figure 6. Mid-IR spectrum region of 2,3 butanedione adsorbed on γ-Al_2O_3. The temperature-dependent development of convoluted features associated with a conjugated product is outlined by the dashed box.

The nature of adsorbed 2,3 butanedione suggests that the species giving rise to the 1480 – 1580 cm^{-1} feature is formed in surface reactions involving C=O and C=C bonds. This broad feature grew as temperature was increased up to 250 °C **(Figure 6)** and likely contains a conjugated system. In addition, the ν(C-H) region **(Figure S8)** included two bands at 2985 and 2937 cm^{-1} that are attributable to asymmetric and symmetric ν(C-H) modes of adsorbed species, respectively. Aside from a slight decrease in intensity, these bands exhibited no change up to 250°C. There were also no new bands emerging in this region. These observations suggest that the conjugated products formed from 2,3 butanedione possess CH_X groups like those of the reagent. Thus, it is likely that either aldol condensation or carbonyl-olefin metathesis may have occurred **(Scheme 6)**. Aldol condensation would perhaps involve a reaction between the 2,3 butanedione diketone and enol tautomers to form a 3,5-dihydroxy-3-methylheptane-2,6-dione intermediate. As with the previously discussed condensation reaction pathways, the intermediate herein may readily dehydrate to form a final 5-hydroxy-3-methylhept-3-ene-2,6-dione product. It may also be possible that the diketone and enol may interact via a carbonyl olefin exchange.[61] The corresponding chain propagation step would result in a 3-hydroxy-4-methylhex-3-ene-2,5-dione. In principle, this species could undergo further exchanges with adsorbed 2,3 butanedione to form elongated, conjugated polymers which could explain the broadness of the 1480—1580 cm^{-1} feature. There was no development in the 1480-1580 cm^{-1} region for adsorbed 3,4 hexanedione, implying that the respective enol does not subsequently react on γ-Al_2O_3.

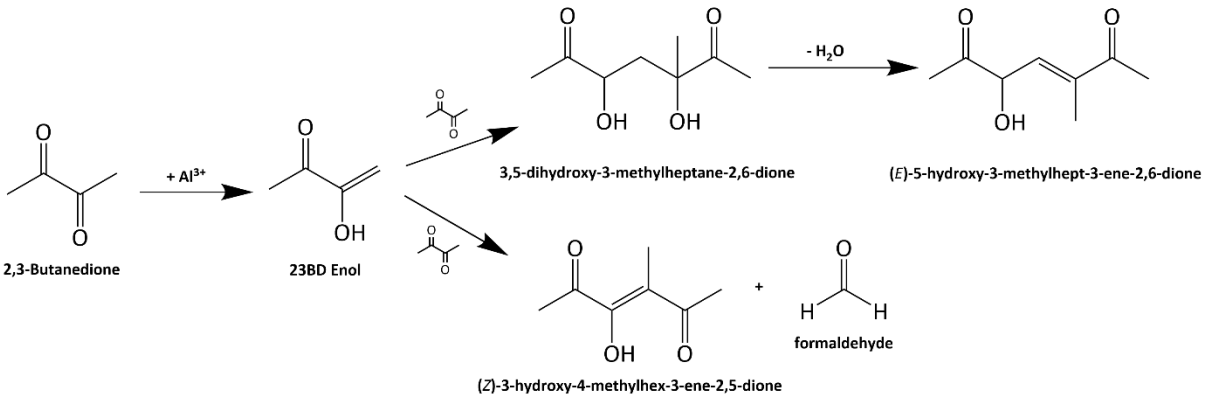

Scheme 6. 2,3 Butanedione reactions on γ-Al_2O_3 up to 250 °C under HV

Table 5. IR band assignments for 2,3 butanedione and 3,4 hexanedione adsorption on γ-Al_2O_3 under HV at 50 – 250 °C. Arrows depict frequency shifts at higher temperatures.

General Vibrational Mode	2,3 Butanedione Adsorption			3,4 Hexanedione Adsorption		
	2,3 Butanedione	C=C Products	Notes	3,4 Hexanedione	C=C Products	Notes
ν(C=O)				1776		Physisorbed 34HD
	1759 → 1755		Free C=O of bound 23BD			
				1745		Free C=O of bound 34HD
	1725 → 1729		23BD on Lewis Acid site			
	1711		H-bonded 23BD		1712	H-bonded 34HD
		1681 → 1676	Free C=O of 23BD enol		1685	Free C=O of 34HD Enol
ν(C=C)					1650	34HD Enol on Lewis Acid site
		1630	23BD enol on Lewis Acid site			
		1600	H-bonded 23BD Enol		1599	H-bonded 34HD Enol
		1480 – 1580	Conjugated product (not deconvoluted)			
δ(CH)		1445			1450	
	1425 → 1418					
	1405				1408	
	1374				1381	
	1357				1358	
					1358	
	1345					
					1336	
					1279 → 1282	
	1225				1232	
	1198				1192	
ν(C-O)	1183					
	1157 → 1163				1150	
	1135				1128	
	1113					
	1083					

2,5 Hexanedione

The IR spectra of γ-Al_2O_3-adsorbed 2,5 hexanedione **(Figure 7)** showed notable absorbance within the 1500 – 1800 cm^{-1} range. While the lack of temperature-dependent development may suggest that no reactions occurred with increasing temperature, the positions of the bands at 1632 and 1585 cm^{-1} suggest that the γ-diketone was quite reactive on γ-Al_2O_3 even at 50 °C and was almost entirely converted into a new, conjugated product with a ν(C=C) mode. The band at 1705 cm^{-1}, which decreased with increasing temperature, was assigned to the ν(C=O) mode of small amounts of weakly adsorbed or unconverted 2,5 hexanedione. The diminishing of this band was attributed to further conversion or desorption.

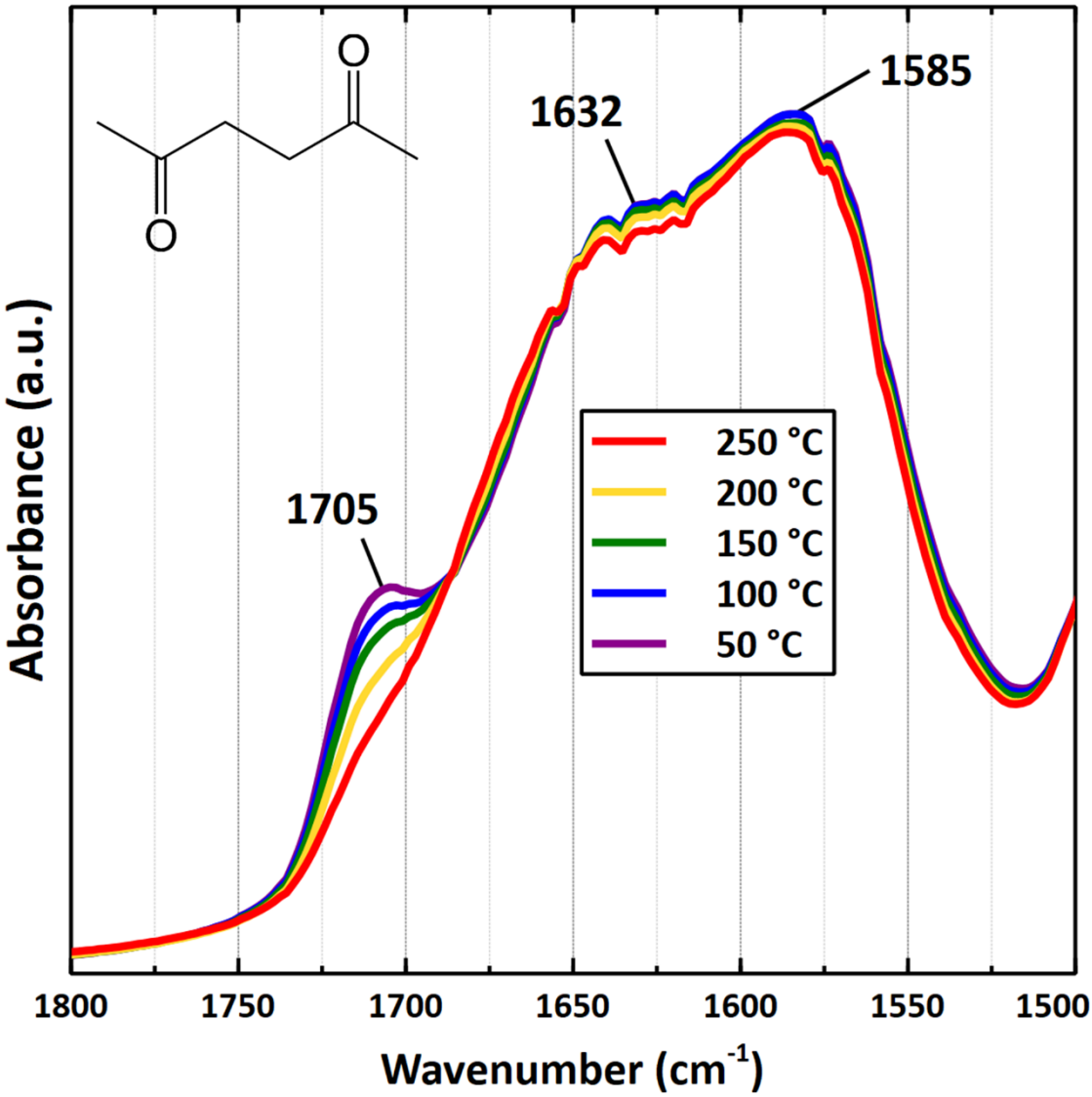

Figure 7. Infrared spectra (ν(C=O) region) of 2,5 hexanedione adsorbed on γ-Al_2O_3 (prepared via ex-situ impregnation) during TPD experiments from 50 to 250 °C.

The presence of a conjugated product suggested that an aldol reaction occurred with the γ-diketone. However, given the insufficient vapor pressure of the diketone and immobility of the chemisorbed enol, it is highly improbable that reactions occurred between the diketone and enol tautomers as previously observed with the other di/ketones. Therefore, the spectra appear to reflect a product formed by an intramolecular aldol condensation in which the alkene

group on one side of the surface enol performed a nucleophilic attack on the free carbonyl on the opposing side **(Scheme 7)**. Following sequential dehydration, this would result in 3-methylcyclopent-2-en-1-one (3M2CP). To corroborate this, a separate TPD experiment was performed with 3M2CP in which the reagent was impregnated ex-situ on γ-Al_2O_3 **(Figure S9)**. Because the IR spectra are very similar throughout the whole 1000 – 2000 cm^{-1} region, we concluded that 3M2CP is the most abundant surface species with aldol condensation as the dominating surface reaction.

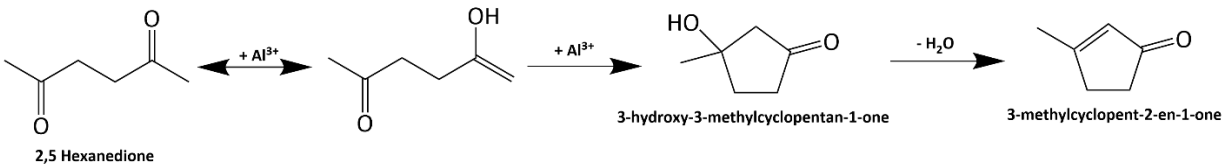

Scheme 7. Reactions of 2,5 Hexanedione on γ-Al_2O_3.

Density functional Theory

The lowest energy configurations for adsorbed diketone species provide insight into how these molecules bind to a γ-Al_2O_3 surface **(Figure 8)**. Our results indicate that each of the diketones, regardless of the positioning of the carbonyl groups, bind to an Al^{3+} site via a carbonyl oxygen atom. The calculated Al^{3+}-O=C angles **(Table S2)** are suggestive of σ-bonding. Other studies that focused on interactions between carbonyls and Lewis acids showed that σ-bonds form via donation of oxygen lone pairs.[62] Each diketone appears bound as a monodentate species, in which the second carbonyl vector is angled away from the surface.

This corroborates the IR spectra interpretation of adsorbed 2,3 butanedione, the only diketone that seemingly avoided enolization at low temperatures, in which two different ν(C=O) modes, one free and one bound, were identified. It is difficult to say the same for the other diketones given their propensity to convert almost completely as low as 50 °C.

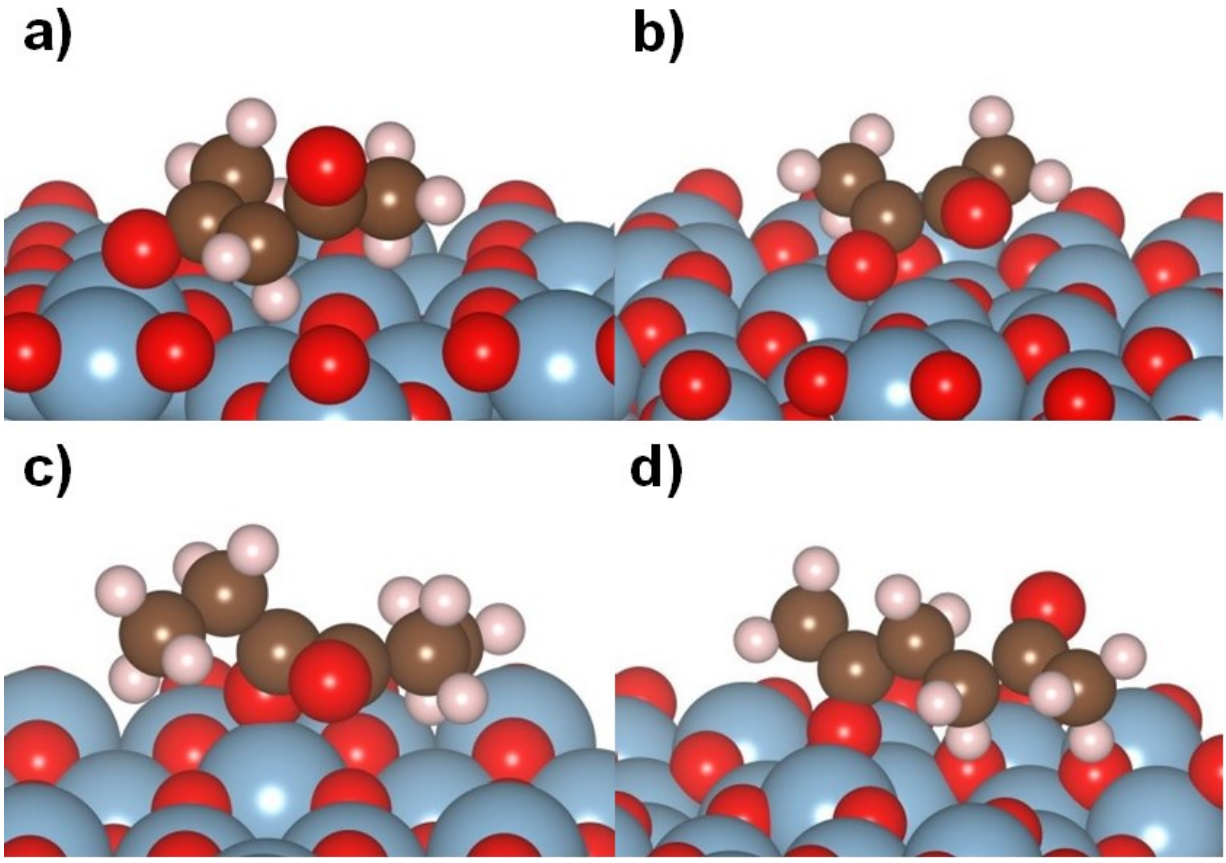

Figure 8. Lowest energy configurations of γ-Al_2O_3-adsorbed **a)** 2,4 pentanedione, **b)** 2,3 butanedione, **c)** 3,4 hexanedione, **d)** 2,5 hexanedione.

The lowest binding energies for diketones adsorbed to γ-Al_2O_3 were calculated with respect to that of adsorbed acetone **(Table 6)**. Binding energies specific to either tetrahedrally or octahedrally coordinated Al^{3+} are presented in Table S3. In this convention negative numbers

mean stronger binding energy than acetone and positive numbers mean weaker binding energy than acetone. Relative binding energies were lower for each diketone when adsorbed to tetrahedrally coordinated sites, with the exception of 2,3 butanedione. However, in the case of 2,3 butanedione the difference in binding energies for the different sites was only 0.07 eV, suggesting that binding in both tetrahedral and octahedral sites is possible. The energetic preference for adsorption to tetrahedrally coordinated sites could be due to the enhanced Lewis acidity of these sites, compared to that of octahedral sites,[63-64] increased exposure (reduced steric hinderance),[65] and electrostatic repulsion between surface oxygen and diketone alkyl chains. The α-diketones exhibited the highest relative binding energies of +0.44 and +0.26 eV for 2,3 butanedione and 3,4 hexanedione, respectively, suggesting that diketones bind less strongly to γ-Al_2O_3 when the carbonyls are directly adjacent. Adsorbed 2,5 hexanedione had a lower relative binding energy of -0.26 eV while adsorbed 2,4 pentanedione was even lower at -0.64 eV, suggesting the latter blinds the strongest. However, the latter calculation does not account for the instantaneous mesomerism observed in the IR spectrum which is perhaps an essential step for stabilizing the surface species. While van der Waals interactions could explain some of the observed differences in binding energy, their contribution is expected to be < 0.1 eV for organic adsorbates on inorganic oxide surfaces.[66] Ultimately there was no clear trend between intramolecular carbonyl distance and binding energies of the adsorbed species. However, the 0.18 eV difference in binding energies between 2,3 butanedione and 3,4 hexanedione suggests the longer alkyl groups of the latter α-diketone are responsible for weakening the bond with γ-Al_2O_3. This is possibly due to the additional sterics of longer alkyl groups along with their greater repulsion from the oxide surface. The Al-O bond distances and

Al-O=C bond angles **(Table S2)** were also obtained from the configurations but presented no apparent trends.

Table 6. DFT-calculated binding energies for γ-Al_2O_3-adsorbed diketones, relative to that of acetone.

Adsorbate	**$E_{Relative\ Binding}$ (eV)**
Acetone	0
2,4 Pentanedione	-0.64
2,3 Butanedione	0.44
3,4 Hexanedione	0.26
2,5 Hexanedione	-0.26

Discussion

The surface chemistry of molecules with multiple functional groups is determined by complex tradeoffs between possible surface interactions of different parts of the molecule.[67-69] The set of di/ketones in this study is chosen to isolate the influence of different structural features on its surface reactions on the Lewis acid sites of γ-Al_2O_3. While reaction pathways were proposed herein for adsorbed di/ketones, further analytical techniques would be required to assess the exact selectivity of the different products as well as potential by-products that were not observed in the IR spectra. The following sections will highlight the roles of hydroxyl groups, length of sorbate alkyl chains, the intramolecular carbonyl distance of diketones and speculations regarding solvent effects by co-adsorbed water.

Acetone is the ideal benchmark ketone reactant given its structural symmetry and simplicity and therefore served as an adequate basis for comparison when studying the adsorption of reactions of more complex di/ketones. Aldol condensation of acetone into

mesityl has been studied extensively on Lewis acidic materials.[19, 43-44, 70] It is also widely accepted that the alkene group of the enol tautomer performs a nucleophilic attack on the carbonyl of a nearby ketone.[71] However, there was little presence of acetone and no observable evidence of its enol tautomer on γ-Al_2O_3 as low as 50 °C. Rather, the deconvoluted IR spectra suggested that mesityl oxide was largely present and that aldol condensation occurs very readily with the simple ketone reagent.

Steric and electronic effects of hydroxyl groups

The presence of hydroxyl groups adds additional complexity to surface reactions of ketones. Upon adsorption, hydroxyacetone demonstrated more stability and resistance to the reaction. Increasing temperatures up to 250 °C seemed to initiate some extent of aldol condensation given by decreasing intensity of the 1718 cm^{-1} hydroxyacetone ν(C=O) band and emergence of 1692, 1588, and 1531 cm^{-1} bands assigned to the ν(C=O) of both 35DH and 15DH, ν(C=C) of 35DH, and ν(C=C) of 15DH, respectively. In acidic environments, hydroxyacetone enolization into the prop-1-ene-1,2 diol intermediate should be more prevalent given the greater inclination for C-H bond cleavage to occur on the hydroxyl carbon.[50] Therefore, the 35HD condensation product should be prevalent on the surface compared to the 15DH alternative as seen on another study regarding hydroxyacetone adsorption on γ-Al_2O_3. This is corroborated by a consistently larger ν(C=C) band integral for the former species at all temperatures up to 250 °C. Nevertheless, hydroxyacetone remained the dominant surface

species according to the strong 1718 cm^{-1} ν(C=O) band suggesting that alcohol groups adjacent to the carbonyl group hinder enolization.

As electron donors, alcohol groups should also prove obstructive for the condensation step. By increasing the overall electron density around the carbonyl group, the ketone should be consequentially shielded from a nucleophilic attack by an enol. While this was partially overcome at higher temperature, no aldol condensation was observed during the adsorption of dihydroxyacetone. This may be partially due to insufficient enolization activity. The molecular enetriol has been observed to act more as an intermediate in the interconversion of dihydroxyacetone and glyceraldehyde; however only in basic (triethylamine) solutions.[72] However, relevant literature also suggests that other competing reactions may occur more readily on γ-Al_2O_3. For instance, it is known that Lewis acids can catalyze the dehydration of dihydroxyacetone (once isomerized into glyceraldehyde or via dimeric intermediate) into pyruvaldehyde,[52, 73] which was observed as a surface species in the IR spectra herein. At temperatures of 50 – 250 °C, the carbonyl group of dihydroxyacetone seemed completely shielded, thus allowing the formation of pyruvic acid to dominate. At temperatures higher than 250 °C, greater conversion of adsorbed dihydroxyacetone into pyruvaldehyde is expected.

The IR spectra herein have suggest that acetone, hydroxyacetone, and dihydroxyacetone can each react on the Lewis acid sites of γ-Al_2O_3 at low temperatures. The contribution of aldol self-condensation reactions, however, becomes less as the carbonyl group becomes surrounded by adjacent hydroxyl groups due to electronic shielding effects, competing reactions, and stricter reaction conditions.

Influence of alkyl group length

While potential mechanisms have been identified herein for the surface chemistry of 2,3 butanedione on γ-Al_2O_3, there remains the question of why the same aldol condensation or metathesis reactions do not appear to occur with 3,4 hexanedione. The dominant, unchanging band at 1650 cm^{-1} suggests that the larger adsorbed α-diketone tautomerizes much more readily than the smaller one at a temperature as low as 50 °C. Yet, there were no absorbance bands within the 1480 – 1580 cm^{-1} region of this spectrum to suggest the formation of a conjugated product nor did they appear as the temperature is increased to 250 °C. There could be a couple of reasons for the lack of reactivity by adsorbed 3,4 hexanedione. Firstly, 3,4 hexanedione is expected to form a trisubstituted alkene group upon enolization, while 2,3 butanedione forms a vinylidine alkene group. The ν(C=C) frequencies of these bonds are generally similar and difficult to distinguish in adsorption spectra.[41] However, previous theoretical studies have illustrated trends in the free energy of hydrogenation to show that trisubstituted alkenes are generally more stable than vinylidene alkenes.[74] This trend should still hold true even with the adjacent electron-withdrawing oxygen atom interacting with a Lewis acid site. Therefore, the trisubstituted alkene of the 3,4 hexanedione is expected to be less reactive towards aldol condensation or metathesis. Secondly, sterics may also play a critical role in the kinetic resistance of the larger α-diketone. Not only should less of the bulkier molecule adsorb to the same surface area, but the ethyl groups of 3,4 hexanedione, as opposed to the methyl groups of 2,3 butanedione, may sterically obstruct the nucleophilic attack on one surface enol by another. As a result of both alkene stability and ethyl group sterics, larger

aliphatic α-diketones may readily enolize upon adsorption to γ-Al_2O_3 yet resist further steps of the aldol condensation reaction pathway.

Intramolecular interactions of carbonyl groups and their effect on the formation of surface species

The IR spectra of surface species from each diketone in this study demonstrated unique surface reactions on γ-Al_2O_3: intermolecular aldol condensation of 2,3 butanedione, enolization of 3,4 hexanedione, mesomerism of 2,4 pentanedione, and intramolecular aldol condensation of 2,5 hexanedione. Given this diversity of surface phenomena, it is difficult to establish trends based on the spectroscopic evidence alone.

Low energy configurations in DFT models **(Figure 8)** revealed that the α-, β-, and γ-diketones bind to γ-Al_2O_3 via the oxygen atom of one carbonyl group. Regardless of intramolecular carbonyl distance, the other carbonyl points away from the surface and does not engage in a strong interaction. For diketones, it was shown that the two carbonyls exhibit intramolecular repulsion and that this interaction decreases significantly with increasing distance between the functional groups, although still present in γ-diketones.[75-76] As shown with various α-dicarbonyls, this intramolecular repulsion results in the trans-conformation being highly dominant over the cis-conformation for the free molecules.[59] For 2,3 butanedione, the only diketone to resist immediate reaction upon adsorption to γ-Al_2O_3, both the DFT conformation and IR spectra suggested that with one carbonyl group immobilized and bound to the surface, the other will point away from the surface; not necessarily forming a perfect trans-

conformation. In a similar study involving the adsorption of aliphatic diketones, Cross and Rochester interpreted their IR spectrum of SiO_2-adsorbed 2,5 hexanedione as evidence of a bidenate surface species.[60] However, the adsorption was performed in CCl_4 solutions and a less acidic SiO_2 surface would perhaps exhibit less repulsion against the alkyl groups of adsorbed di/ketones.

Impact of an aqueous phase

The presence of large quantities of water, inherent to many biomass conversion processes, is expected to have an effect on the discussed surface reactions on γ-Al_2O_3. Firstly, γ-Al_2O_3 transforms into a hydrated boehmite (AlOOH) phase with severely reduced surface area and Lewis acidity under liquid water at 200 °C.[77] In theory, this should decrease the di/ketone adsorption capacity of the catalyst support and impede enolization. Surface hydroxyls and adsorbed H_2O are very stable on Al_2O_3 surfaces at high temperatures and pressures and are unlikely to be displaced by most of the di/ketones studied herein, because they are less prone to forming multidentate surface species that could outcompete water for surface sites. Polyols, however, have shown potential in stabilizing γ-Al_2O_3 surfaces under hot, pressurized aqueous environments via formation of a protective adlayer.[77] Studying the reactions observed herein under the aqueous phase and improving the hydrothermal stability of γ-Al_2O_3 with chelating, mesomeric diketones, such as 2,4 pentanedione and potentially other β-diketones, may be of interest for future studies.

Conclusion

Understanding the reactions and trends of adsorbed di/ketones on Lewis acidic materials such as γ-Al_2O_3 is essential for the chemical industry. Deconvolution and interpretation of IR bands of the ν(C=O) and ν(C=C) modes of adsorbed species revealed aldol condensation to be the most common surface reaction and as well as the effects of adjacent hydroxyl groups and the molecular size. Hydroxyl groups adjacent to the carbonyl group act as electron shields against nucleophilic attacks necessary for C-C bond formation. This was overcome with higher temperatures (up to 250 °C) for adsorbed hydroxyacetone, while isomerization dominated at all temperatures for adsorbed dihydroxyacetone. While 2,3 butanedione showed enolization and aldol condensation activity with increasing temperatures, the larger α-diketone, 3,4 hexanedione, formed a stable enol likely due to the increased steric hinderance of larger alkyl groups as well as the greater thermodynamic stability of the trisubstituted C=C bond of the respective enol. Other unique surface phenomena were observed for 2,4 pentanedione (mesomerism) and 2,5 hexanedione (intramolecular aldol condensation), making it difficult to establish trends based on experimental data. DFT calculations suggested stable diketone surface species bind to γ-Al_2O_3 in a monodentate orientation with one carbonyl bound to the surface and one pointing away from the surface. Adsorbed species with relative binding energies on the lower side of this range (acetone and 2,5 hexanedione) should be expected to undergo the full aldol condensation mechanism more readily. This study has improved understanding of di/ketone surface chemistry on Lewis-acidic materials which may facilitate progress in various fields from prebiotic chemistry to sustainable industrial chemistry.

Supporting Information

DFT simulation super cell, adsorbate orientations and geometrical parameters, IR spectra and band assignments for vapor phase di/ketones, IR spectra corroborating claims and assignments made regarding adsorbed di/ketones and products from surface reactions.

Acknowledgements

This project was funded primarily by grants CHE-1764304 and CHE-1764296 from the U.S. National Science Foundation. Additional COVID-19 Disruption GRA funds were generously provided by the Georgia Institute of Technology through the Higher Education Emergency Relief Funding program. The authors would also like to personally thank Dr. Giada Innocenti for writing the Python code used herein to deconvolute IR spectra.

References

1. Mokhtari, M.; Archer, E.; Bloomfield, N.; Harkin-Jones, E.; McIlhagger, A., A Review of Electrically Conductive Poly(Ether Ether Ketone) Materials. *Polym. Int.l* **2021**, *70*, 1016-1025.
2. Shukla, D.; Negi, Y. S.; Uppadhyaya, J. S.; Kumar, V., Synthesis and Modification of Poly(Ether Ether Ketone) and Their Properties: A Review. *Polym. Rev.* **2012**, *52*, 189-228.
3. Morris, R. H., Asymmetric Hydrogenation, Transfer Hydrogenation and Hydrosilylation of Ketones Catalyzed by Iron Complexes. *Chem. Soc. Rev.* **2009**, *38*, 2282-2291.
4. Mäki-Arvela, P.; Simakova, I. L.; Murzin, D. Y., One-Pot Amination of Aldehydes and Ketones over Heterogeneous Catalysts for Production of Secondary Amines. *Catal. Rev.: Sci. Eng.* **2021**, 1-68.

5. Kel'in, A. V.; Maioli, A., Recent Advances in the Chemistry of 1, 3-Diketones: Structural Modifications and Synthetic Applications. *Curr. Org. Chem.* **2003**, *7*, 1855-1886.
6. Samanta, S.; Zhao, C.-G., Asymmetric Direct Aldol Reaction of 1,2-Diketones and Ketones Mediated by Proline Derivatives. *Tetrahedron Lett.* **2006**, *47*, 3383-3386.
7. Trueba, M.; Trasatti, S. P., γ-Alumina as a Support for Catalysts: A Review of Fundamental Aspects. *European journal of inorganic chemistry* **2005**, *2005*, 3393-3403.
8. Prins, R., On the Structure of γ-Al_2O_3. *J. Catal.* **2020**, *392*, 336-346.
9. Dry, M. E., Practical and Theoretical Aspects of the Catalytic Fischer-Tropsch Process. *Appl. Catal. A: Gen.l* **1996**, *138*, 319-344.
10. Cortright, R. D.; Davda, R. R.; Dumesic, J. A., Hydrogen from Catalytic Reforming of Biomass-Derived Hydrocarbons in Liquid Water. *Nature* **2002**, *418*, 964-967.
11. Pineda, M.; Palacios, J. M., The Performance of a γ-Al_2O_3 Catalyst for the Claus Reaction at Low Temperature in a Fixed Bed Reactor. *Appl. Catal. A: Gen.* **1996**, *136*, 81-96.
12. Knözinger, H.; Bühl, H.; Kochloefl, K., The Dehydration of Alcohols on Alumina: Xiv. Reactivity and Mechanism. *J. Catal.* **1972**, *24*, 57-68.
13. Avery, N. R., EELS Identification of the Adsorbed Species from Acetone Adsorption on Pt (111). *Surf. Sci.* **1983**, *125*, 771-786.
14. Lin, Y.; Ji, H.; Shen, Z.; Jia, Q.; Wang, D., Enhanced Acetone Sensing Properties of Co_3O_4 Nanosheets with Highly Exposed (111) Planes. *J. Mater. Sci.: Mater. Electron.* **2016**, *27*, 2086-2095.
15. Würger, T.; Heckel, W.; Sellschopp, K.; Müller, S.; Stierle, A.; Wang, Y.; Noei, H.; Feldbauer, G., Adsorption of Acetone on Rutile TiO_2: A DFT and FTIR Study. *The J. Phys. Chem. C* **2018**, *122*, 19481-19490.
16. Vannice, M. A.; Erley, W.; Ibach, H., A RAIRS and HREELS Study of Acetone on Pt(111). *Surf. Sci.* **1991**, *254*, 1-11.
17. Gao, J.; Teplyakov, A. V., Chemical Transformations of Acetone on ZnO Powder. *J. Catal.* **2014**, *319*, 136-141.
18. Johnston, S. M.; Mulligan, A.; Dhanak, V.; Kadodwala, M., The Bonding of Acetone on Cu(111). *Surf. Sci.* **2004**, *548*, 5-12.
19. Panov, A.; Fripiat, J., Acetone Condensation Reaction on Acid Catalysts. *J. Catal.* **1998**, *178*, 188-197.
20. Hanson, B. E.; Wieserman, L. F.; Wagner, G. W.; Kaufman, R. A., Identification of Acetone Enolate on γ-Alumina: Implications for the Oligomerization and Polymerization of Adsorbed Acetone. *Langmuir* **1987**, *3*, 549-555.
21. Qi, G.; Chu, Y.; Wang, Q.; Wang, X.; Li, Y.; Trébosc, J.; Lafon, O.; Xu, J.; Deng, F., Gem-Diol-Type Intermediate in the Activation of a Ketone on Sn-β Zeolite as Studied by Solid-State NMR Spectroscopy. *Angew. Chem. Int. Ed.* **2020**, *59*, 19532-19538.
22. Senanayake, S. D.; Gordon, W. O.; Overbury, S. H.; Mullins, D. R., Adsorption and Reaction of Acetone over CeOx(111) Thin Films. *J. Phys. Chem. C* **2009**, *113*, 6208-6214.
23. Connor, P. A.; Dobson, K. D.; McQuillan, A. J., New Sol-Gel Attenuated Total Reflection Infrared Spectroscopic Method for Analysis of Adsorption at Metal Oxide

Surfaces in Aqueous Solutions. Chelation of TiO_2, ZrO_2, and Al_2O_3 Surfaces by Catechol, 8-Quinolinol, and Acetylacetone. *Langmuir* **1995**, *11*, 4193-4195.
24. Blanck, S.; Martí, C.; Loehlé, S.; Steinmann, S. N.; Michel, C., (Dis)Similarities of Adsorption of Diverse Functional Groups over Alumina and Hematite Depending on the Surface State. *J. Chem. Phys.* **2021**, *154*, 084701.
25. Sadeghian Lemraski, M.; Nadimi, E., Acetone Gas Sensing Mechanism on Zinc Oxide Surfaces: A First Principles Calculation. *Surf. Sci.* **2017**, *657*, 96-103.
26. Lin, F.; Wang, H.; Zhao, Y.; Fu, J.; Mei, D.; Jaegers, N. R.; Gao, F.; Wang, Y., Elucidation of Active Sites in Aldol Condensation of Acetone over Single-Facet Dominant Anatase TiO2 (101) and (001) Catalysts. *JACS Au* **2021**, *1*, 41-52.
27. Innocenti, G., Giadainnocenti/Ftir_Analyzer. GitHub, 2021.
28. Digne, M.; Sautet, P.; Raybaud, P.; Euzen, P.; Toulhoat, H., Use of DFT to Achieve a Rational Understanding of Acid–Basic Properties of γ-Alumina Surfaces. *J. Catal.* **2004**, *226*, 54-68.
29. Kresse, G.; Hafner, J., *Ab Initio* Molecular Dynamics for Liquid Metals. *Phys. Rev. B* **1993**, *47*, 558-561.
30. Kresse, G.; Furthmüller, J., Efficiency of Ab-Initio Total Energy Calculations for Metals and Semiconductors Using a Plane-Wave Basis Set. *Computat. Mater. Sci.* **1996**, *6*, 15-50.
31. Kresse, G.; Furthmüller, J., Efficient Iterative Schemes for *Ab Initio* Total-Energy Calculations Using a Plane-Wave Basis Set. *Phys. Rev. B* **1996**, *54*, 11169-11186.
32. Hacene, M.; Anciaux-Sedrakian, A.; Rozanska, X.; Klahr, D.; Guignon, T.; Fleurat-Lessard, P., Accelerating Vasp Electronic Structure Calculations Using Graphic Processing Units. *J. Computat. Chem.* **2012**, *33*, 2581-2589.
33. Hutchinson, M.; Widom, M., Vasp on a Gpu: Application to Exact-Exchange Calculations of the Stability of Elemental Boron. *Comput. Phys. Commun.* **2012**, *183*, 1422-1426.
34. Mortensen, J. J.; Hansen, L. B.; Jacobsen, K. W., Real-Space Grid Implementation of the Projector Augmented Wave Method. *Phys. Rev. B* **2005**, *71*, 035109.
35. Kresse, G.; Joubert, D., From Ultrasoft Pseudopotentials to the Projector Augmented-Wave Method. *Phys.Rev. B* **1999**, *59*, 1758-1775.
36. Perdew, J. P.; Burke, K.; Ernzerhof, M., Generalized Gradient Approximation Made Simple. *Phys. Rev. Lett.* **1996**, *77*, 3865-3868.
37. Grimme, S.; Antony, J.; Ehrlich, S.; Krieg, H., A Consistent and Accurate Ab Initio Parametrization of Density Functional Dispersion Correction (DFT-D) for the 94 Elements H-Pu. *J. Chem. Phys.* **2010**, *132*, 154104.
38. Grimme, S.; Ehrlich, S.; Goerigk, L., Effect of the Damping Function in Dispersion Corrected Density Functional Theory. *J. Comput. Chem.* **2011**, *32*, 1456-1465.
39. Monkhorst, H. J.; Pack, J. D., Special Points for Brillouin-Zone Integrations. *Phys.l Rev. B* **1976**, *13*, 5188-5192.
40. Hare, B. J.; Garcia Carcamo, R. A.; Xie, T.; Meza-Morales, P. J.; Getman, R. B.; Sievers, C., Active Sites and Effects of Co-Adsorbed H_2o on Isolated Methanol Dehydrogenation over Pt/Γ-Al_2o_3. *J. Catal.* **2021**, *402*, 218-228.

41. Colthup, N. B.; Daly, L. H.; Wiberly, S. E., *Introduction to Infrared and Raman Spectroscopy*, Third edition ed.; Academic Press, Inc. and Harcourt Brace Jovanavich, Inc.: San Diego, CA, USA, 1990.
42. Busca, G., The Surface of Transitional Aluminas: A Critical Review. *Catal. Tod.* **2014**, *226*, 2-13.
43. Zaki, M. I.; Hasan, M. A.; Al-Sagheer, F. A.; Pasupulety, L., Surface Chemistry of Acetone on Metal Oxides: Ir Observation of Acetone Adsorption and Consequent Surface Reactions on Silica−Alumina Versus Silica and Alumina. *Langmuir* **2000**, *16*, 430-436.
44. Panov, A.; Fripiat, J. J., An Infrared Spectroscopic Study of Acetone and Mesityl Oxide Adsorption on Acid Catalyst. *Langmuir* **1998**, *14*, 3788-3796.
45. Gray Jr, H.; Rasmussen, R.; Tunnicliff, D., The Infrared and Ultraviolet Absorption Spectra of Two Isomers of Mesityl Oxide. *J. Am. Chem. Soc.* **1947**, *69*, 1630-1631.
46. Najmi, S.; So, J.; Stavitski, E.; McDermott, W. P.; Lyu, Y.; Burt, S. P.; Hermans, I.; Sholl, D. S.; Sievers, C., In-Situ IR Spectroscopy Study of Reactions of C_3 Oxygenates on Heteroatom (Sn, Mo, and W) Doped Bea Zeolites and the Effect of Co-Adsorbed Water. *ChemCatChem* **2021**, *13*, 445-458.
47. Faba, L.; Díaz, E.; Ordóñez, S., Gas Phase Acetone Self-Condensation over Unsupported and Supported Mg–Zr Mixed-Oxides Catalysts. *Appl. Catal. B: Environ.* **2013**, *142-143*, 387-395.
48. Ramis, G.; Lorenzelli, V., Adsorption and Oligomerization of Isobutene on Oxide Catalyst Surfaces. A Fourier-Transform Infrared Study. *J. Chem. Soc., Faraday Trans. 1* **1989**, *85*, 137-146.
49. Koichumanova, K.; Vikla, A. K. K.; Cortese, R.; Ferrante, F.; Seshan, K.; Duca, D.; Lefferts, L., In Situ Atr-Ir Studies in Aqueous Phase Reforming of Hydroxyacetone on Pt/ZrO_2 and Pt/AlO(OH) Catalysts: The Role of Aldol Condensation. *Appl. Catal. B: Environ.* **2018**, *232*, 454-463.
50. Yaylayan, V. A.; Harty-Majors, S.; Ismail, A. A., Monitoring Carbonyl−Amine Reaction and Enolization of 1-Hydroxy-2-Propanone (Acetol) by FTIR Spectroscopy. *J. Agric. Food Chem.* **1999**, *47*, 2335-2340.
51. Hossain, M. A.; Mills, K. N.; Molley, A. M.; Rahaman, M. S.; Tulaphol, S.; Lalvani, S. B.; Dong, J.; Sunkara, M. K.; Sathitsuksanoh, N., Catalytic Isomerization of Dihydroxyacetone to Lactic Acid by Heat Treated Zeolites. *Appl. Catal. A: Gen.* **2021**, *611*, 117979.
52. Innocenti, G.; Papadopoulos, E.; Fornasari, G.; Cavani, F.; Medford, A. J.; Sievers, C., Continuous Liquid-Phase Upgrading of Dihydroxyacetone to Lactic Acid over Metal Phosphate Catalysts. *ACS Catal.* **2020**, *10*, 11936-11950.
53. Temprado, M.; Roux, M. V.; Umnahanant, P.; Zhao, H.; Chickos, J. S., The Thermochemistry of 2,4-Pentanedione Revisited: Observance of a Nonzero Enthalpy of Mixing between Tautomers and Its Effects on Enthalpies of Formation. *J. Phys. Chem. B* **2005**, *109*, 12590-12595.
54. Kytökivi, A.; Rautiainen, A.; Root, A., Reaction of Acetylacetone Vapour with Γ-Alumina. *J. Chem. Soc., Faraday Trans.* **1997**, *93*, 4079-4084.

55. Dickie, S. A.; McQuillan, A. J., In-Situ Infrared Spectroscopic Studies of Adsorption Processes on Boehmite Particle Films: Exchange of Surface Hydroxyl Groups Observed Upon Chelation by Acetylacetone. *Langmuir* **2004**, *20*, 11630-11636.
56. Dismukes, J.; Jones, L.; Bailar Jr, J. C., The Measurement of Metal-Ligand Bond Vibrations in Acetylacetonate Complexes. *J. Phys. Chem.* **1961**, *65*, 792-795.
57. Tsyganova, E. I.; Dyagileva, L. M., The Reactivity of Metal B-Diketonates in the Thermal Decomposition Reaction. *Russ. Chem. Rev.* **1996**, *65*, 315.
58. Grimm, S.; Baik, S.-J.; Hemberger, P.; Bodi, A.; Kempf, A. M.; Kasper, T.; Atakan, B., Gas-Phase Aluminium Acetylacetonate Decomposition: Revision of the Current Mechanism by Vuv Synchrotron Radiation. *Phys. Chem. Chem. Phys.* **2021**, *23*, 15059-15075.
59. Profeta, L. T. M.; Sams, R. L.; Johnson, T. J.; Williams, S. D., Quantitative Infrared Intensity Studies of Vapor-Phase Glyoxal, Methylglyoxal, and 2,3-Butanedione (Diacetyl) with Vibrational Assignments. *J. Phys. Chemi. A* **2011**, *115*, 9886-9900.
60. Cross, S. N.; Rochester, C. H., Infrared Study of the Adsorption of Diketones on Silica Immersed in Carbon Tetrachloride. *J. Chem. Soc., Faraday Trans. 1* **1978**, *74*, 2130-2140.
61. Albright, H.; Davis, A. J.; Gomez-Lopez, J. L.; Vonesh, H. L.; Quach, P. K.; Lambert, T. H.; Schindler, C. S., Carbonyl–Olefin Metathesis. *Chem. Rev.* **2021**, *121*, 9359-9406.
62. Román-Leshkov, Y.; Davis, M. E., Activation of Carbonyl-Containing Molecules with Solid Lewis Acids in Aqueous Media. *ACS Catal.* **2011**, *1*, 1566-1580.
63. Hirva, P.; Pakkanen, T. A., The Interaction of Amine Bases on the Lewis Acid Sites of Aluminum Oxide — a Theoretical Study. *Sur. Sci.* **1992**, *277*, 389-394.
64. Zecchina, A.; Platero, E. E.; Areán, C. O., Low Temperature Co Adsorption on Alum-Derived Active Alumina: An Infrared Investigation. *J. Catal.* **1987**, *107*, 244-247.
65. De Vito, D. A.; Gilardoni, F.; Kiwi-Minsker, L.; Morgantini, P.-Y.; Porchet, S.; Renken, A.; Weber, J., Theoretical Investigation of the Adsorption of Methanol on the (110) Surface of γ-Alumina. *J. Mol. Struct.: THEOCHEM* **1999**, *469*, 7-14.
66. Tillotson, M. J.; Brett, P. M.; Bennett, R. A.; Grau-Crespo, R., Adsorption of Organic Molecules at the Tio_2(110) Surface: The Effect of Van Der Waals Interactions. *Surf. Sci.* **2015**, *632*, 142-153.
67. Sievers, C.; Noda, Y.; Qi, L.; Albuquerque, E. M.; Rioux, R. M.; Scott, S. L., Phenomena Affecting Catalytic Reactions at Solid–Liquid Interfaces. *ACS Catal.* **2016**, *6*, 8286-8307.
68. Lee, J.-K.; Kung, M. C.; Kung, H. H., Cooperative Catalysis: A New Development in Heterogeneous Catalysis. *Top. Catal.* **2008**, *49*, 136-144.
69. Kung, H. H.; Kung, M. C., Inspiration from Nature for Heterogeneous Catalysis. *Catal. Lett.* **2014**, *144*, 1643-1652.
70. Zaki, M. I.; Hasan, M. A.; Pasupulety, L., Surface Reactions of Acetone on Al_2o_3, Tio_2, Zro_2, and Ceo_2: Ir Spectroscopic Assessment of Impacts of the Surface Acid−Base Properties. *Langmuir* **2001**, *17*, 768-774.
71. Perrin, C. L.; Chang, K.-L., The Complete Mechanism of an Aldol Condensation. *J. Org. Chem.* **2016**, *81*, 5631-5635.

72. A. Yaylayan, V.; Harty-Majors, S.; A. Ismail, A., Investigation of Dl-Glyceraldehyde–Dihydroxyacetone Interconversion by Ftir Spectroscopy. *Carbohydr. Res.* **1999**, *318*, 20-25.
73. Yamaguchi, S.; Yabushita, M.; Kim, M.; Hirayama, J.; Motokura, K.; Fukuoka, A.; Nakajima, K., Catalytic Conversion of Biomass-Derived Carbohydrates to Methyl Lactate by Acid–Base Bifunctional γ-Al_2O_3. *ACS Sust. Chem. Eng.* **2018**, *6*, 8113-8117.
74. Silva de Freitas, G. R.; Firme, C. L., New Insights into the Stability of Alkenes and Alkynes, Fluoro-Substituted or Not: A DFT, G4, Qtaim and Gvb Study. *J. Mol. Model.* **2013**, *19*, 5267-5276.
75. Dougherty, D.; Brint, P.; McGlynn, S., Photoelectron Spectroscopy of Carbonyls. Lone-Pair Interactions In. Alpha.-,. Beta.-,. Gamma.-, And. Delta.-Dicarbonyls. *J. Am. Chem. Soc.* **1978**, *100*, 5597-5603.
76. Eriks, K.; Hayden, T. D.; Yang, S. H.; Chan, I. Y., Crystal and Molecular Structure of Biacetyl (2,3-Butanedione), (H_3CO)2, at -12 and -100.Degree.C. *J. Am. Chem. Soc.* **1983**, *105*, 3940-3942.
77. Ravenelle, R. M.; Copeland, J. R.; Kim, W.-G.; Crittenden, J. C.; Sievers, C., Structural Changes of γ-Al_2O_3-Supported Catalysts in Hot Liquid Water. *ACS Catal.* **2011**, *1*, 552-561.

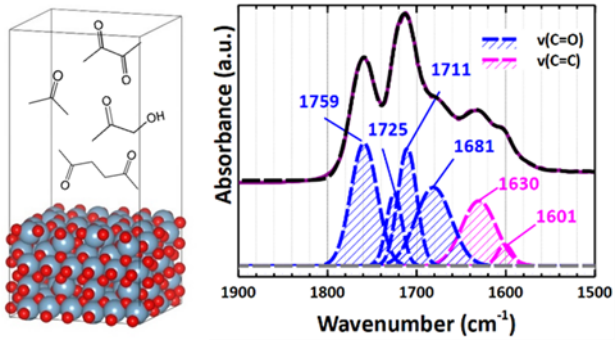

TOC Graphic